Final Report—Phase II

ANALYSIS OF ATS PHOTOGRAPHS USING A SPECIALLY DESIGNED ELECTRONIC CONSOLE

Prepared for:

NATIONAL AERONAUTICS AND SPACE ADMINISTRATION
GODDARD SPACE FLIGHT CENTER
GREENBELT, MARYLAND 20771

STANFORD RESEARCH INSTITUTE
Menlo Park, California 94025 · U.S.A.

STANFORD RESEARCH INSTITUTE
Menlo Park, California 94025 · U.S.A.

Final Report—Phase II

Covering the Period 8 October 1970 to 8 October 1971

ANALYSIS OF ATS PHOTOGRAPHS USING A SPECIALLY DESIGNED ELECTRONIC CONSOLE

By: ROY H. BLACKMER, JR. WILLIAM VIEZEE RUSSELL M. TRUDEAU

Prepared for:

NATIONAL AERONAUTICS AND SPACE ADMINISTRATION
GODDARD SPACE FLIGHT CENTER
GREENBELT, MARYLAND 20771

Contracting Officer: Henry Arista
Technical Monitor: William E. Shenk

CONTRACT NAS5-21086 MOD. NO. 1

SRI Project 8244

Approved by:

R. T. H. COLLIS, *Director*
Atmospheric Sciences Laboratory

RAY L. LEADABRAND, *Executive Director*
Electronics and Radio Sciences Division

ABSTRACT

Three areas of investigation were conducted using cloud-motion measurements made on the SRI/NASA Electronic Display System. The studies dealt with computations of relative vorticity from measured cloud motions, relationship of cloud motion to changes in circulation, and comparisons of cloud motions with cloud sizes.

The derived vorticity was compared with NMC analyses and also with similar kinematic quantities obtained from rawins. The comparisons showed low correlation between absolute values of relative vorticity computed from mid-level cloud motions and 500-mb NMC values, but showed good positive correlation with vorticity computed from concurrent rawinsonde data for the 700-mb level.

In the investigation of the relationship of cloud motion to changes in circulation, measured cloud motions in a deepening cyclone were compared with those in a filling cyclone. During the filling stage, the cloud motion speeds averaged higher than during the deepening stage. Also during the filling stage, the cloud directions departed less from the rawinsonde wind direction but showed larger variation from the rawinsonde wind speed than during the filling stage.

In the comparison of cloud motion with cloud size, measurements of the motions of clouds of various sizes were compared with wind direction and speed from rawins. No correlations were found between cloud size and altitude of best agreement with measured winds or between cloud size alone and amount of deviation from wind direction or speed. However, there was a tendency for clouds larger than 400 nmi^2 that were increasing

in size to show speeds greater than the wind speed and such large clouds that were decreasing in size moved slower than the wind speed.

CONTENTS

ILLUSTRATIONS

TABLES

ACKNOWLEDGMENTS

The authors wish to acknowledge the contributions of E. J. Wiegman and R. G. Hadfield, Research Meteorologists, who made the measurements of cloud motions used in this study. They also acknowledge the efforts of R. L. Mancuso, Senior Research Meteorologist, who computer processed the raw data to put it in a readily usable form for analysis and interpretation.

Mrs. A. G. Burris, Meteorological Assistant, drafted the many figures.

Throughout the study S. M. Serebreny, Manager, Atmospheric Analysis Program, provided guidance and many valuable suggestions.

I INTRODUCTION

This is the second phase of a study in which the SRI/NASA Electronic Display System has been used as an aid in the measurement, interpretation, and analysis of ATS photographs. During the first study Blackmer et al. (1970)* demonstrated the capabilities and limitations of the system by performing three diverse tasks:

- Evaluating identification of cloud-height and measured cloud displacements at large angles of view (using only ATS cloud photographs) through the use of the equipment and comparing the results to those made by a second investigator working with the same data using ATS photographs and concurrent ESSA satellite photographs.
- Comparing the distribution of cloud types and heights determined from cloud-motion measurements of ATS III photographic data to the cloud cover viewed by Apollo 6 between the east coast of the United States and the west coast of Africa on 4 April 1968.
- Evaluating and comparing growth rates and movements of cumulonimbus anvils to the occurrence and severity of the attendant weather and with the wind shear at appropriate levels.

---

*References are listed at the end of the report.

In this second phase of the study, objectives were specified and subdivided into a series of tasks to determine the extent to which cloud motions measured with the SRI/NASA Electronic Display system are related to various atmospheric conditions. These objectives and tasks are listed below.

A. Objectives

The objectives of this study have been to investigate:

- The utility of kinematic analyses derived from cloud motion vectors obtained on the electronic console to studies of cyclone development, and from this to determine the relationship between cloud motion and horizontal wind.
- The relationship of cloud motion to cloud size.
- The relationship of cloud motion to changes in circulation.

B. Research Tasks

A number of research tasks have been specified for each objective. These were as follows:

1. Objective I: Cloud-Motion Vector/Vorticity Relation

Task 1: Using the electronic console, derive cloud motion vectors corresponding to low-level and high-level clouds in an intensifying extratropical cyclone system.

Task 2: Determine vorticity and divergence patterns for low- and high-level clouds and compare these

analyzed patterns to corresponding cloud patterns. Assess whether the general magnitudes of the kinematic quantities are reasonable, using accepted standards available in the literature.

Task 3: If the patterns and magnitudes are acceptable, compute the vertical motions. Relate spatial and temporal variations to the variations in satellite-observed cloud patterns and the development of the cyclone. If patterns and/or magnitudes are not acceptable, determine the cause of the discrepancy.

2. Objective II: Relationship of Cloud Motion to Cloud Size

Task 1: Select a series of ATS pictures over the Caribbean, including the BOMEX area, and derive cloud motion vectors for the selected series of cloud samples.

Task 2: Compare the vector motions with the wind reports nearest in time and distance to the measured cloud, using:

(1) The vector difference between cloud motion and wind at the level of best fit in the conventional wind data.

(2) The vector difference between the cloud motion and the wind at the 850-mb level, for low clouds and the wind at the 300-mb level, for high clouds. The adjudication of the cloud level will be done subjectively.

Task 3: Where possible, develop correlations between cloud motion and conventional wind.

Task 4: Based on success under Task 3, compare how correlation varies as a function of:

(1) Individual cloud size

(2) Cluster size

(3) Magnitude of wind vector

(4) Weather type.

3. Objective III: Relationship of Cloud Motion to Changes in Circulation

Task 1: Using representative examples of a circulation system, such as a frontal low or easterly wave (to be mutually agreed upon between the Technical Monitor and SRI) that exhibits deepening, filling, and upper air diffluence, obtain the cloud motion vector in various parts of these pressure systems.

Task 2: Compare these cloud-motion vectors to conventional wind data nearest in time and space to the cloud measurement and derive the vector difference between cloud motion and

(1) The wind at the level of best fit

(2) The winds at the 850-mb level (in the case of low clouds) or at the 300-mb level (in the case of high clouds).

Task 3: Ascertain if there are any differences that occur between cloud motion and wind during a deepening

(lowering) pressure change or filling (rising) pressure change that are useful in meteorological analyses. Determine if diffluence aloft is detectable in cloud motion patterns.

C. Method of Approach

To fulfill the requirements of Objectives I and III, available ATS photographs were examined; from these, the period 16 to 18 March 1970 was selected for analysis. The cloud motions were then measured on the SRI/NASA Electronic Display system. The resulting measurements were analyzed using one series of techniques for Objective I and a second series of techniques for Objective III. The analyses for the two objectives were carried out independently by two different groups of investigators.

For Objective I, cloud heights were subjectively assigned on the basis of appearance, relative speed, and position in the synoptic situation in order to assess how well we could do in vorticity computations using only cloud motion vectors without any reference to rawin observations. Whereas in the third objective cloud heights were assigned by comparison of measured cloud motions with wind data from rawinsondes at proximal stations to determine the pressure level at which the cloud motion vectors were closest to the observed wind vectors. This pressure level has been designated the "level of best fit" (LBF) or "level of minimum vector difference" (LMVD).

Work on Objective II required ATS data over the Caribbean, including the BOMEX area. Accordingly, ATS data over this area were examined and four days with usable photographs--12, 13, 26, and 27 July 1969--were selected for analysis. Measurements were made of cloud motions in the vicinity of available rawinsonde stations for comparison of

cloud motion and measured wind. Cloud size, rate of change of size, and orientation of major and minor axes were also measured. Relationships between measured winds and these parameters are presented in Section IV.

II CLOUD MOTION VECTOR/VORTICITY RELATION

A. Background

In recent years, several investigators have reported on the development of techniques for incorporating information derived from satellite cloud pictures into the operational numerical analysis in data-sparse areas (e.g., McClain and Brodrick, 1967). The basic problem is to convert qualitative satellite photographs of clouds and cloud patterns to quantitative data on the wind field or the pressure/height field for input into numerical analysis and prediction.

Using video data from TIROS and ESSA satellites, attempts have been made to develop classification schemes whereby cloud patterns associated with extratropical cyclones are modeled in terms of patterns of dynamic quantities pertinent to cyclone development. For example, the cloud patterns or cloud signatures associated with a developing extratropical cyclone have been divided into various development stages that can be recognized in the satellite photographs. These stages are then related, through modeling, to magnitudes of maximum cyclonic vorticity and to the location of the center of maximum cyclonic vorticity (Brodrick, 1969). Such relations enable a reanalysis of the 500-mb stream-function field in those areas where few or no conventional data are present but where satellite video data show thick, multilayer stratiform cloudiness.

With the advent of the geosynchronous Advanced Technology Satellite (ATS), the speed and direction of the movement of clouds attached to the cloud system of a cyclone can be measured from the daytime series of high-resolution photographs, which are taken 20 to 30 minutes apart. Using ATS data, cloud motions have been shown to represent the winds to about

5 m/s (Serebreny et al., 1970a; Hubert and Whitney, 1971). Smaller errors (3 m/s) have been associated with low clouds assumed to be located at 850 mb; larger errors (8 m/s) have been found for the high clouds assumed to be located at the 300-mb level. The principal hypothesis for the degraded accuracy for the high clouds is the considerable uncertainty regarding cloud height. Future geosynchronous satellites will have window infrared imaging capability to determine cloud top heights more accurately and hopefully reduce the wind/cloud motion differences. A study by Shenk and Kreins (1970) has already investigated the potential improvement of infrared data by tracking clouds from one Numbus 2 orbital pass to the next at high latitudes where substantial data overlap between orbits occurs. The wind/cloud motion comparisons were about the same as those for the ATS data. However, there was no difference in accuracy for low clouds (850-mb) and clouds located between 400 and 500-mb. The explanation for these similar results despite better cloud top height information was probably due to difficulties in relative geographical alignment of the Nimbus radiation field and greater uncertainties in cloud tracking when clouds are viewed at 108-minute intervals instead of the 20 to 30 minutes for ATS.

Fujita et al. (1969) have demonstrated that the dynamic characteristics of tropical disturbances can be clarified by analyzing the associated fields of cloud motion vectors. Fujita et al. computed--and subsequently interpreted--the patterns of relative vorticity and divergence associated with three tropical cyclones in the eastern Pacific from the streamlines and isotachs of the field of low-cloud motion. The present study extends the technique of computing and interpreting kinematic quantities derived from cloud motion vectors associated with an extratropical cyclone. Specifically, the distributions of relative vorticity and derived height fields over an area of deep stratiform cloudiness associated with a developing surface cyclone over the continental United States are computed

from fields of cloud motion vectors. The potential of using such computations as input into numerical analysis and prediction in areas where standard data are sparse or nonexistent is evaluated.

B. Data Selection and Analysis

The period 16 through 18 March 1970, when the subsatellite point of ATS III was at 83°-85°W, was chosen for analysis. This period combined surface cyclogenesis over the continental United States with a series of ATS III cloud photographs that was by no means ideal but definitely superior to other series covering cyclone development during this season.

On 16 March, a frontal cyclone developed in the lee of the Southern Rocky Mountains (Texas Panhandle/Oklahoma/Kansas) and subsequently moved eastnortheast, reaching the East Coast on 18 March. Figure 1 shows a synoptic surface chart, and an ATS cloud-photograph for 17 March. The cloud photograph, which is typical of the series available for the period of analysis, shows the abundance of clouds suitable for middle- and high-level cloud motion determination. Since no significant deepening took place, the cyclone must be considered as a stable frontal wave cyclone.

1. Cloud-Motion Analysis

The feasibility of computing the distribution of vorticity and derived heights from cloud motion vectors depends on a capability to compile and analyze a large volume of cloud motions over the area and level of interest. In the present study, such a capability was provided by the SRI/NASA Electronic Display System, the design and performance of which have been described by Serebreny et al. (1970b). Cloud motions were obtained by tracking on the console cloud elements over time periods from one to three hours. Appropriate cloud elements, selected using criteria similar to those discussed by Hubert and Whitney (1971), were

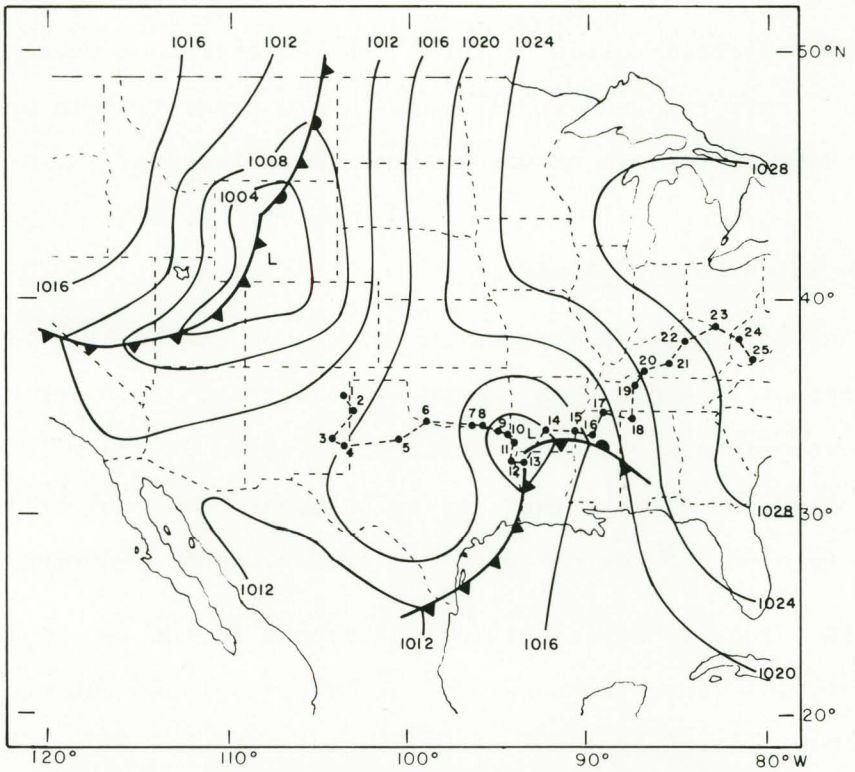

a) SURFACE CHART 1200GMT 17 MARCH 1970 WITH 3 HOURLY POSITIONS OF LOW CENTER FROM 0000GMT 16 MARCH (1) TO 0000GMT 19 MARCH (25)

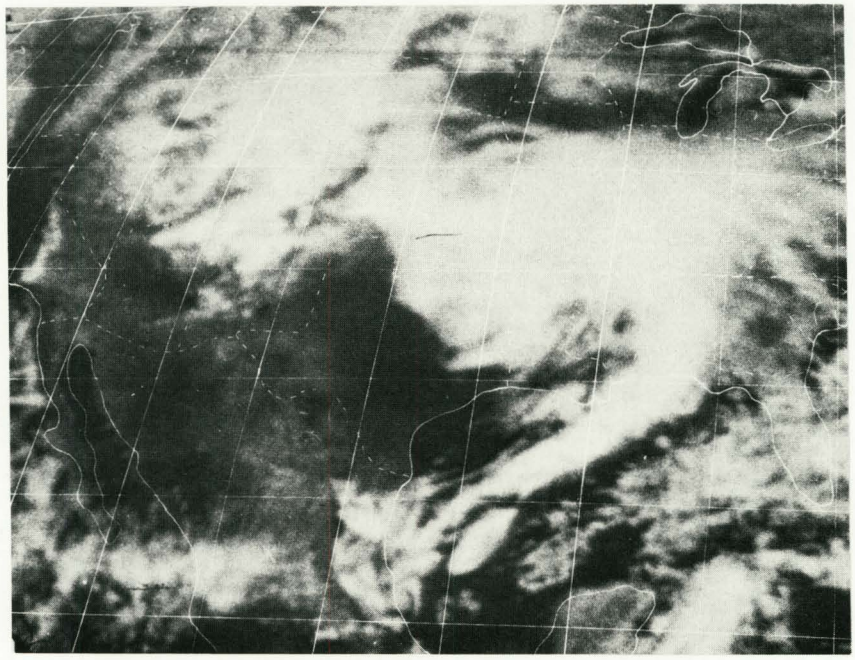

b) ATS PHOTOGRAPH, 2015GMT 17 MARCH 1970

FIGURE 1 FRONTAL CYCLONE SELECTED FOR ANALYSIS

subjectively considered to be "high," "middle," or "low" -level clouds on the basis of their appearance and relative motion.

Because of the thick, layer-type cloudiness associated with the selected storm, most of the clouds in the vicinity of the cyclone were classified as middle or high. Over large areas, the low clouds either could not be observed at all or their characteristic features could not be identified on successive frames. Consequently, only the high- and middle- (mid) level cloud motion fields were analyzed. Table 1 lists the total number of cloud motion vectors obtained from the display system for each day analyzed.

Scan line dropouts limited the number of satellite pictures suitable for processing, thus introducing some variability in the time interval between usable frames. These shortcomings, however, did not seriously affect the measurement of cloud motions in and around the area of the cyclone.

The various steps in the data collection and analysis were as follows. Series of ATS III cloud pictures provided the input to the console. Appropriate cloud elements from these series were tracked over time intervals of one to three hours. Data on the initial and final position of selected cloud features were recorded in the form of x and y cursor values, together with the time period over which the cloud feature was tracked. These values were used as input to the ATSWIND* computer program, which computes the cloud direction, speed, latitude, longitude, and the midpoint of the time interval over which the cloud element was followed. The output from the ATSWIND program provides the input to a second computer program, which:

---

*Initially supplied by NESS, NOAA, and modified at SRI.

Table 1

CLOUD MOTION VECTORS OBTAINED FROM ELECTRONIC DISPLAY SYSTEM
FOR THE PERIOD 16 THROUGH 18 MARCH 1970

Date (1970)	Period of ATS Coverage (GMT)	Number of Available Frames	Time between Successive Frames (min)	Minimum Tracking Time Used (min)	Number of Cloud Motion Vectors		
					Low	Middle	High
16 March	15:55-17:39	3	52	52	22	155	206
17 March	15:10-20:47	16	22	66	16	148	247
18 March	15:33-20:46	12	26	78	51	287	199

- Prints out on a Mercator projection of the continental United States all cloud motion vectors for each day and each level.

- Converts the initial cloud motion vector field to a 2.5° latitude × 2.5° longitude grid-point analysis. The objective procedure by which this is accomplished (Endlich et al., 1971) is quite similar to the techniques used in hand analyses. For example, the spatial distribution of the observed cloud motion vectors is examined to reject individual cloud motions that show a large inconsistency with adjacent motions. An interpolation procedure is used to assign a value to each grid point.

- Computes from the continuous field of grid-point vectors the corresponding patterns of relative vorticity.

- Computes a geopotential height field (hereinafter referred to as the balanced height) from the "balance equation," using the field of cloud motion vectors as wind vectors (Mancuso, 1967).

2. Error Analysis

To measure cloud motions, the meteorologist/operator at the console, using the time-lapse mode, selects advected cloud elements that remain identifiable through a number of frames of the recorded sequence. The display system uses two electronically generated, movable cursors giving x and y values of a Cartesian coordinate system as the basic measuring device. The x and y cursor values, taken at the initial and final location of a cloud element, are used to compute the distance a cloud element moves during a given time period. The earth distance corresponding to one cursor unit on the displayed ATS photograph depends on

the magnification of the displayed photograph and on the angles of view of that portion of the photograph being viewed. For the area and magnification used in our study, the maximum earth distance of a cursor unit represents about 7 nmi. This results in a random error in both x and y location of a cloud element, which at most would be about ± 3.5 nmi. A reasonable estimate of the 50 percent probable error would be about one half of this or ± 1.8 nmi.

In addition to the cursor error, there is also a random definition error: Because of poor picture quality or time changes in cloud shapes, a cloud element can only be pinpointed to a certain degree of accuracy, which includes the effects of human judgments. Assuming the definition error to be identical in magnitude to the cursor error, the combined probable error in both the x or y location of a cloud element would be ± 2.5 nmi, based on the theory of errors (Beers, 1962). For clouds measured over a one-hour time interval, the corresponding error in both the computed u and v components of the cloud motions would be ± 3.5 kts, while the error in vorticity would be $\pm 0.7 \times 10^{-5} s^{-1}$ when computed from cloud motions having identical heights. Systematic errors in the cloud motions may also exist due to photographic distortion and registration. The magnitude of these errors is not known, but considerable care was taken to register the photographs with regard to local terrain features in order to minimize registration errors.

The present major uncertainty in using cloud motions to measure winds is in the subjective assignment of cloud height. In this study, cloud motions were categorized as low, mid, or high level, depending mainly on the various cloud characteristics that allows one to distinguish the associated cloud types (such as cirrus, cumulus, stratus, and the like). The division into these three height-categories was made based on studies by Serebreny et al. (1969) and by Shenk and Kreins (1970) in which it was found that the levels at which the cloud motion most closely

approximates the wind direction and speed tended to cluster at three altitude levels. Of course, one would expect the mean altitudes of the three height categories to vary with latitude. For example, in the high-level category (which includes cirrus-type clouds), the true height should differ significantly for cirrus associated with a polar jet stream and cirrus associated with a subtropical jet stream. Evidence of such height differences in our analyses were obtained in this study.

C. Discussion of Results

1. Distribution of Relative Vorticity and Balanced Heights

a. Middle-Level

Figures 2, 3, and 4 show the ATS photographs and the vorticity distributions computed from the mid-level cloud velocities for 16, 17, and 18 March, respectively. The vorticity analyses are assumed valid at approximately 1800 GMT, which is near the mid-point of the period for which ATS data were available. Also reproduced are the initial field of cloud motion vectors as obtained from the available ATS data, and the NMC analyses of vorticity* (valid approximately six hours after the time of the cloud-motion analyses). For purposes of comparing patterns, the contours of the NMC analyses are transferred to the Mercator projection used by our computer program and are relabeled in terms of relative vorticity by subtracting a value of $8 \times 10^{-5} s^{-1}$ for the vorticity of the earth (Coriolis parameter). This value corresponds to 35°N, the mean latitude of our area of analysis. The location of the surface low-pressure center is indicated on each chart by the symbol (x).

---

*Absolute vorticity (initial, 500-mb) prepared by the staff of the U.S. Weather Bureau's National Meteorological Center.

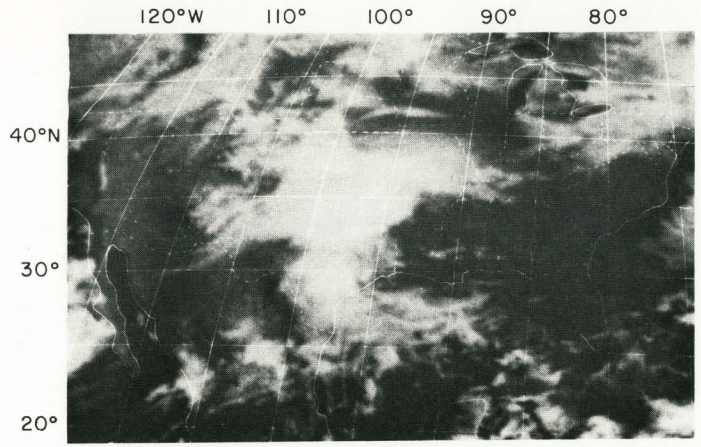

a) ATS PHOTOGRAPH 1739GMT

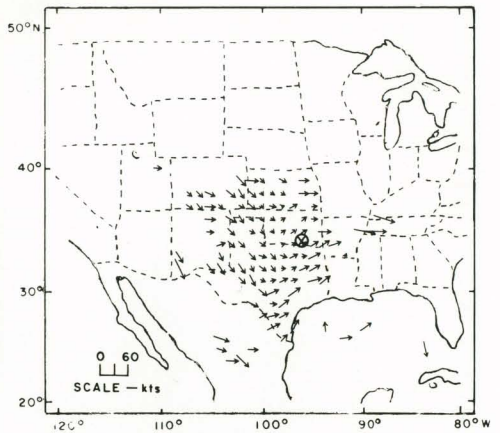

b) MID-LEVEL CLOUD MOTIONS 1555 to 1739GMT

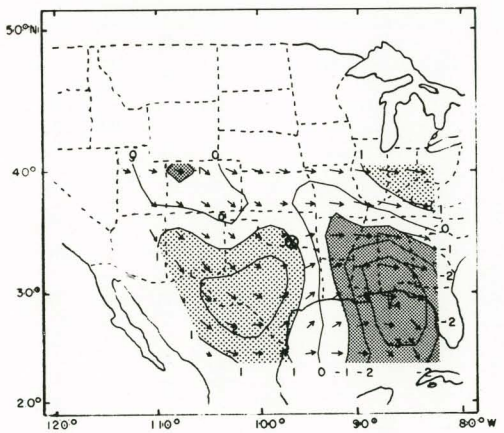

c) RELATIVE VORTICITY OF MID-LEVEL CLOUD MOTIONS ($10^{-5}sec^{-1}$, Positive Values-Cyclonic)

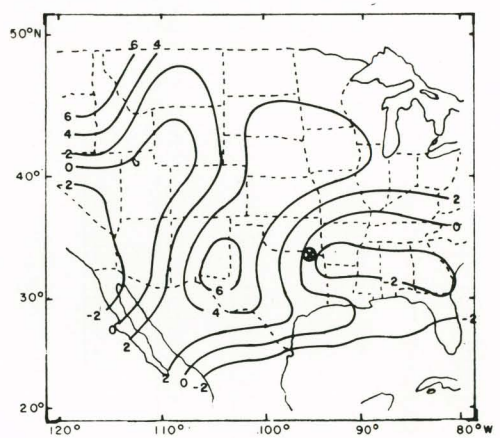

d) RELATIVE VORTICITY FROM 500mb NMC ANALYSIS FOR 0000GMT 17 MARCH ($10^{-5}sec^{-1}$, Positive Values-Cyclonic)

FIGURE 2 CLOUD COVER, CLOUD MOTIONS, AND RELATIVE VORTICITY FOR 16 MARCH 1970

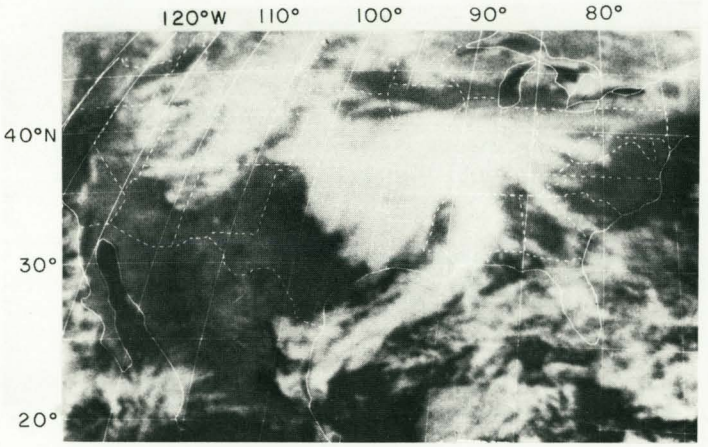

a) ATS PHOTOGRAPH 1804GMT

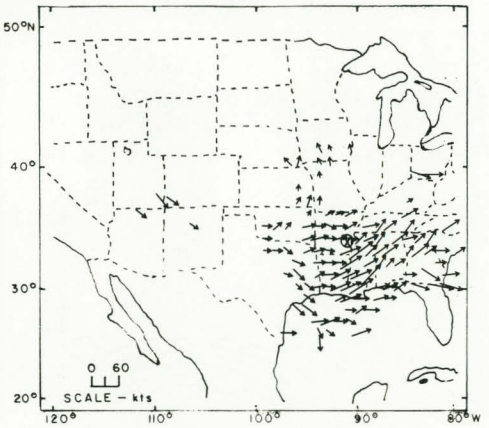

b) MID-LEVEL CLOUD MOTIONS
1510 to 2047GMT

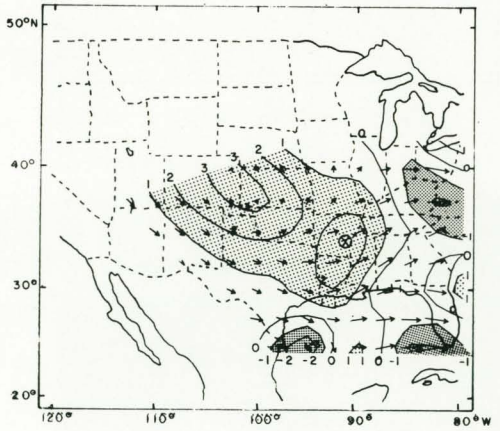

c) RELATIVE VORTICITY OF MID-LEVEL CLOUD MOTIONS ($10^{-5}sec^{-1}$, Positive Values-Cyclonic)

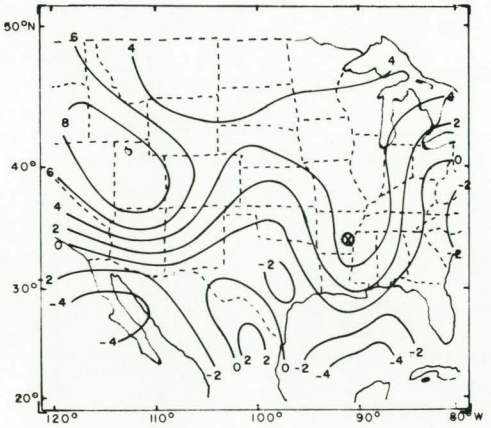

d) RELATIVE VORTICITY FROM 500mb NMC ANALYSIS FOR 0000GMT 18 MARCH ($10^{-5}sec^{-1}$, Positive Values-Cyclonic)

FIGURE 3 CLOUD COVER, CLOUD MOTIONS, AND RELATIVE VORTICITY FOR 17 MARCH 1970

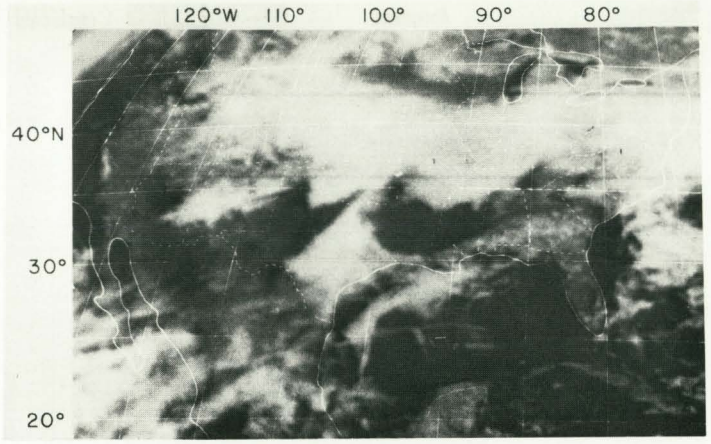

a) ATS PHOTOGRAPH 1835GMT

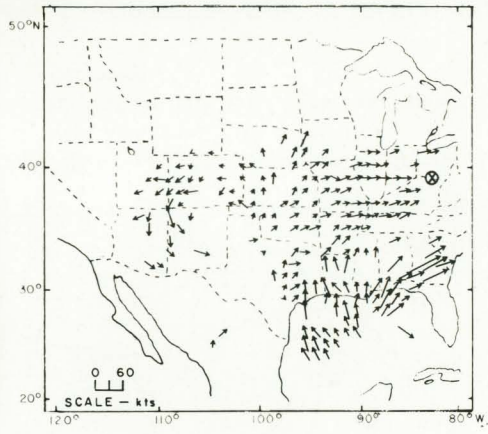

b) MID-LEVEL CLOUD MOTIONS
1533 to 2046GMT

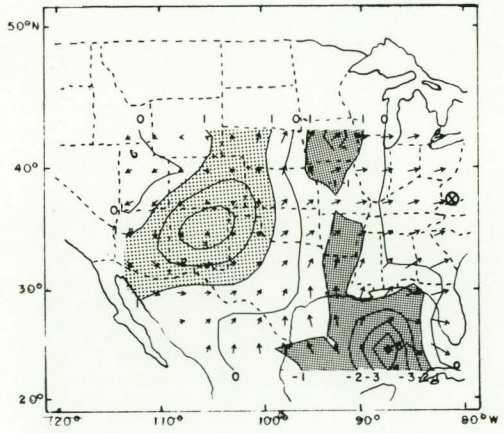

c) RELATIVE VORTICITY OF MID-LEVEL CLOUD MOTIONS (10^{-5} sec^{-1}, Positive Values - Cyclonic)

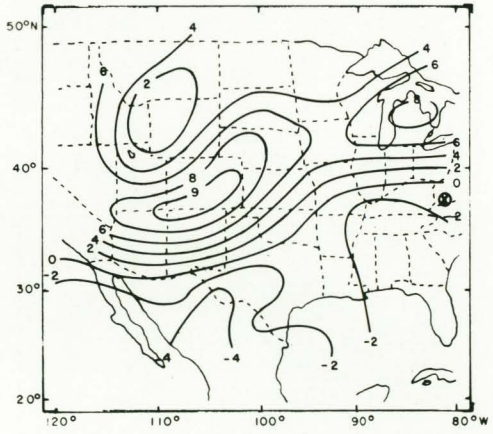

d) RELATIVE VORTICITY FROM 500mb NMC ANALYSIS FOR 0000GMT 19 MARCH (10^{-5} sec^{-1}, Positive Values-Cyclonic)

FIGURE 4 CLOUD COVER, CLOUD MOTIONS, AND RELATIVE VORTICITY FOR 18 MARCH 1970

In our analyses, areas with relative cyclonic vorticity $\geq 1 \times 10^{-5} s^{-1}$ and relative anticyclonic vorticity $\leq -1 \times 10^{-5} s^{-1}$ are shaded. Because of the probable error of approximately $\pm 0.7 \times 10^{-5} s^{-1}$, the shaded areas represent reliable results as to the sign of the vorticity. In areas where no cloud motion vectors could be determined because of the absence of clouds or identifiable cloud elements, interpolation was used to obtain a continuous grid-point vector field (see, for example, the area of Texas and New Mexico on 18 March).

On 16 and 17 March, the areas of maximum relative cyclonic and anticyclonic vorticity associated with the surface cyclone in the analyses of the mid-level cloud velocities are reflected in the NMC analyses of 0000 GMT 17 and 18 March. The absence of large cyclonic vorticity over the center of the surface cyclone in both the NMC and our analysis on 18 March is indicative of the filling of the cyclone, which occurred after 2100 GMT 17 March. However, renewed cyclogenesis in the lee of the southern Rocky Mountains in the NMC analysis of 19 March is clearly indicated by the appearance of relatively large cyclonic vorticity in the cloud-motion analysis on 18 March. On 17 March, the cloud velocities show relatively large cyclonic vorticity near Kansas-Colorado, a feature that is absent in the NMC analyses. It is likely that our computations in that area are inaccurate because of the absence of actual cloud-motion measurements. The indicated vorticity distribution was computed from cloud motions obtained by interpolation using the few available motion vectors over New Mexico and southwestern Colorado. The large vorticity gradient over Missouri in the NMC analysis of Figure 4(d) is not present in the cloud-motion analysis of Figure 4(c). Examination of the wind field in this area showed that wind speed and cyclonic shear increased significantly from 1200 GMT 18 March to 0000 GMT 19 March. However, of more importance is that the wind speed and shear at the 700-mb level were not that large. In fact the 700-mb wind field showed a col area in

southern Iowa. Evidence that the mid-level cloud motion vorticity corresponds better to the 700- than to the 500-mb level is presented below. Figures 2, 3, and 4 suggest a good qualitative comparison between the vorticity pattern computed from the cloud velocities and those present in the NMC analyses.

In order to make a more quantitative comparison for each day of the three-day period, the grid-point values of relative vorticity computed from the mid-level cloud motion vectors (CMV) were correlated with values of vorticity read off the NMC analyses at the same gridpoints. In order to convert absolute vorticity to relative vorticity, the NMC values were reduced by the exact Coriolis parameter rather than the mean value used in the pattern comparisons. It was found that correlations improved by averaging the NMC values for 1200 GMT and 0000 GMT. Figure 5 shows the resulting scatter diagrams with the linear regression of relative vorticity NMC (y coordinate) on relative vorticity CMV (x coordinate). Thus, the regression lines are fitted to the data points so as to be able to estimate values of NMC vorticity from computed values of CMV vorticity. Except on 16 March, the overall correlations are not very high [linear correlation coefficients (R) of 0.70, 0.46, and 0.45 for 16, 17, and 18 March, respectively] and there is considerable data scatter around the regression lines as indicated by the values of the standard error of estimate (SEE). The thin lines parallel to the regression line are drawn at a vertical (y direction) distance equal to ± one standard error of estimate or ± 1 standard deviation of the dependent variable (relative vorticity NMC). Close to 68 percent of the points in the scatter diagram lie between these two lines. It is obvious that if the linear regression model is applied, rather large errors could be involved if relative vorticity NMC were predicted from relative vorticity values computed from cloud motion vectors. For example, the sign of the NMC vorticity could not be estimated with any confidence for a range of CMV

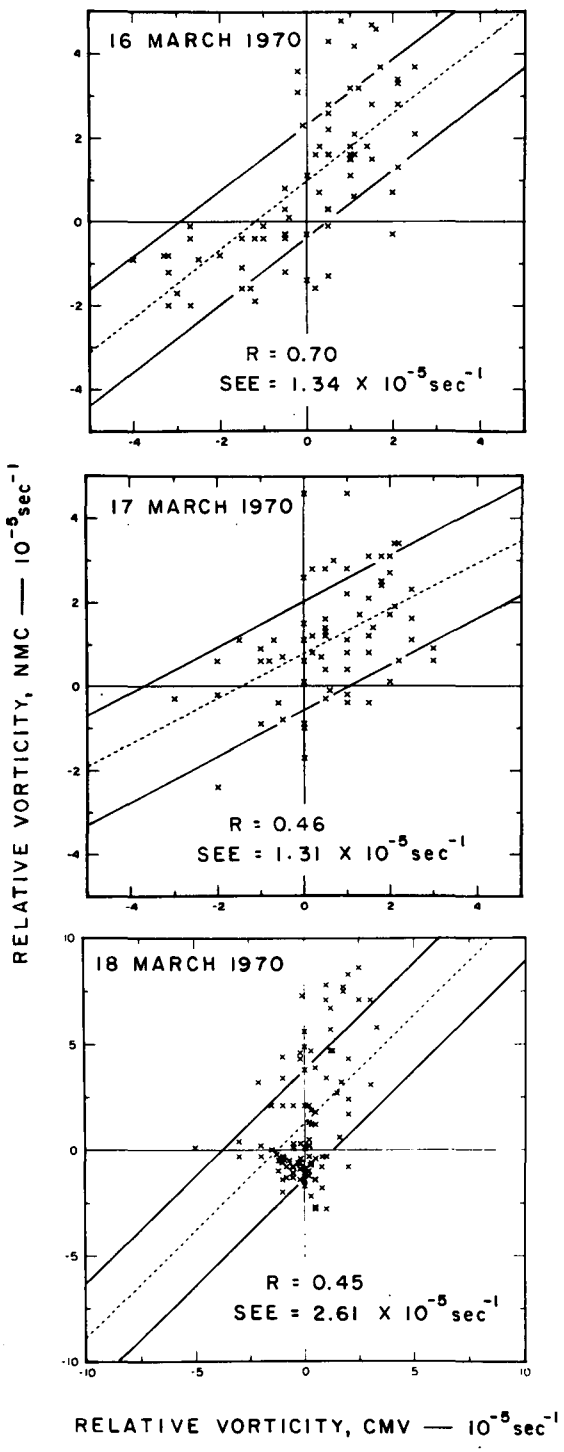

FIGURE 5 SCATTER DIAGRAMS SHOWING LINEAR REGRESSION OF 500 mb RELATIVE VORTICITY FROM NMC (averaged for 1200 GMT and 0000 GMT) ON RELATIVE VORTICITY COMPUTED FROM MID-LEVEL CLOUD MOTIONS FOR 16, 17, AND 18 MARCH 1970

values between $+1.0 \times 10^{-5}\ s^{-1}$ and $-3.0 \times 10^{-5}\ s^{-1}$. The fair relation between the absolute value of CMV and NMC vorticity could be attributed to the following:

- While the NMC analyses refer to the 500-mb level, no absolute height can be assigned to our mid-level cloud motions. (Evidence presented later suggests that for this storm the mid-level is closer to 700-mb than to 500-mb.)
- Differences in magnitude between NMC and CMV vorticity may be due to computational differences: NMC vorticity is computed from observed heights, while CMV vorticity is computed from a smoothed grid-point analysis of cloud motions.
- The cloud motions are time averaged whereas the conventional measuresments provide a nearly instantaneous measure of the wind vector.

It was found that extrapolation and interpolation used in our computational program to obtain a continuous field of grid-point values of cloud motion was not responsible for the low correlations.. Such interpolation over New Mexico and Colorado on 17 March could have modified existing horizontal wind shear and streamline curvature to the extent that cyclonic vorticity was reduced compared to the NMC analysis. However, no increase in correlation was evident when the grid-point values in this area were eliminated from the scatter diagram of Figure 5.

Figure 6 shows scatter diagrams of the relative vorticity obtained from the mid-level cloud motions of 17 March and the relative vorticity computed from observed winds at the 700-, 500-, and 400-mb constant-pressure levels. The observed winds were obtained by averaging rawinsonde data at 1200 GMT 17 March and 0000 GMT 18 March, and relative

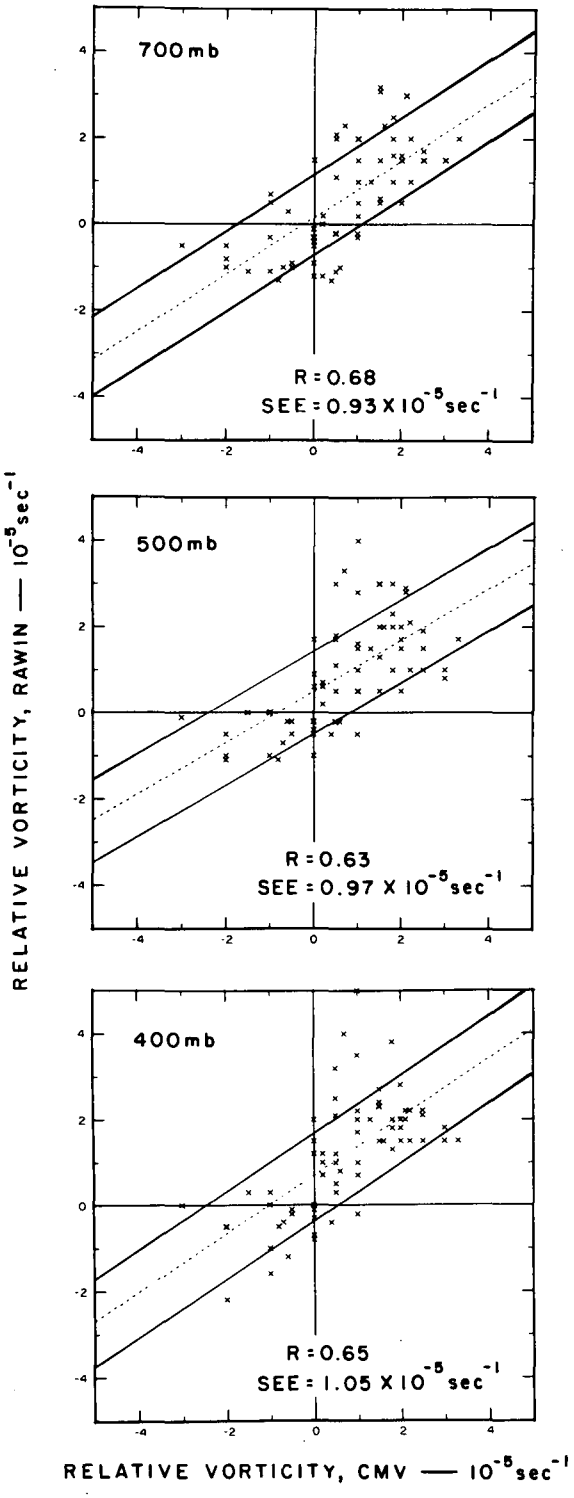

FIGURE 6 SCATTER DIAGRAMS SHOWING THE LINEAR REGRESSION OF RELATIVE VORTICITY COMPUTED FROM RAWINS FOR 700, 500 AND 400 mb (averaged for 1200 GMT and 0000 GMT) ON RELATIVE VORTICITY COMPUTED FROM MID-LEVEL CLOUD MOTIONS FOR 17 MARCH 1970

vorticity was computed from these winds using the same program described earlier. It can be seen that the scatter around the regression lines of Figure 6 is much less than in the comparison with the NMC vorticity of 17 March shown in Figure 5. Correlation coefficients, regression coefficients (slope of regression line), y-axis intercepts, and standard errors of estimates are listed in Table 2 for all three pressure levels and also for the data comparison of 17 March using the NMC vorticity. It should be emphasized that vorticity computed on the basis of the mid-level cloud motion measurements corresponds better to the vorticity derived from the observed winds than to the vorticity obtained from the available NMC analysis. Furthermore, vorticity computations for the 700-mb winds give a slightly better correlation and fit than computations derived from observed winds at higher levels.

Table 2

STATISTICS OF THE LINEAR REGRESSION OF RELATIVE VORTICITY FROM RAWINS ON RELATIVE VORTICITY FROM CMV FOR 17 MARCH 1970

Level	Correlation Coefficient, R	Regression Coefficient	Y-axis Intercept ($10^{-5}s^{-1}$)	Standard Error of Estimate (SEE) ($10^{-5}s^{-1}$)
700-mb	0.68	0.66	0.16	0.93
500-mb	0.63	0.59	0.49	0.97
400-mb	0.65	0.68	0.70	1.05
NMC	0.46	0.53	0.78	1.31

In Figures 7 and 8, isoline analyses of balanced height derived from the mid-level cloud motions on 16, 17, and 18 March (indicated as solid lines) can be compared with corresponding NMC analyses of 700-mb and 500-mb height contours, respectively (indicated as dashed lines). The fields of balanced height are valid at approximately 1800

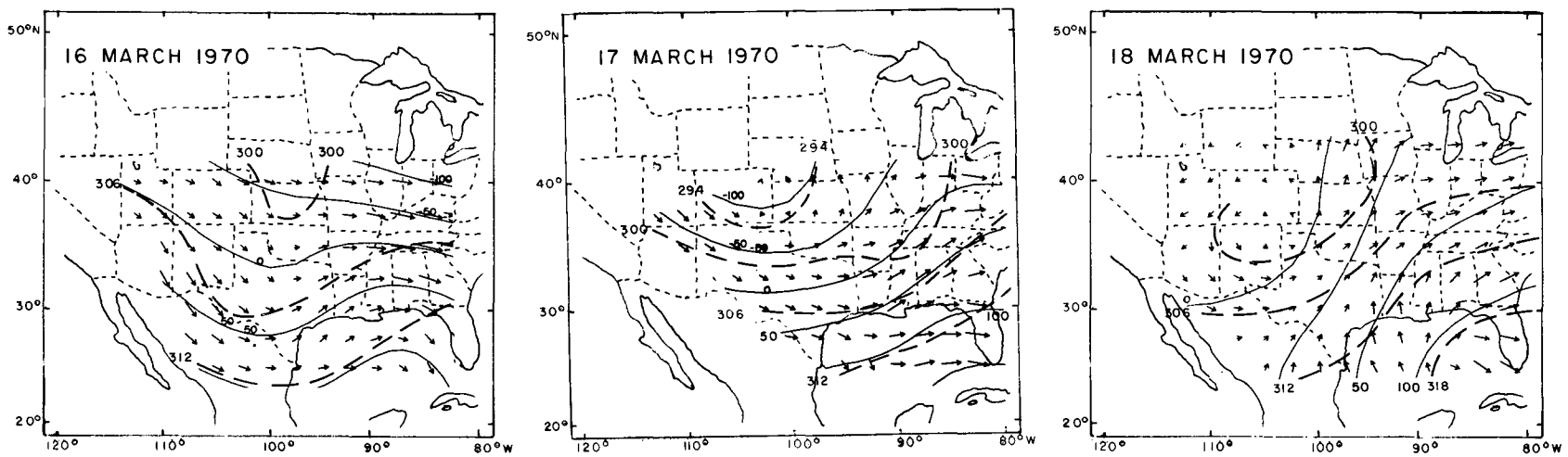

FIGURE 7 COMPARISON BETWEEN RELATIVE VARIATIONS OF BALANCED HEIGHT COMPUTED FROM MID-LEVEL CLOUD MOTIONS (solid lines at intervals of 50 m) FOR 16, 17 MARCH 1970, AND 700 mb HEIGHT CONTOURS FROM NMC AT 0000 GMT FOR 17, 18, AND 19 MARCH 1970 (dashed lines at intervals of 6 decameters). (Grid-point analysis of cloud motion vectors superposed.)

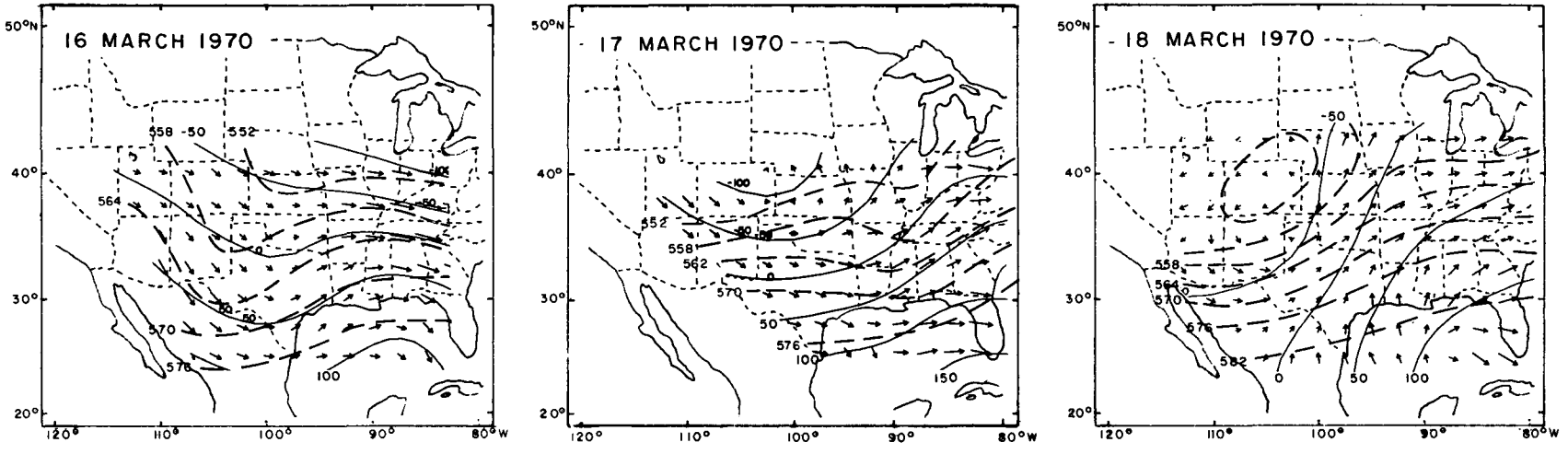

FIGURE 8 COMPARISON BETWEEN RELATIVE VARIATIONS OF BALANCED HEIGHT COMPUTED FROM MID-LEVEL CLOUD MOTIONS (solid lines at intervals of 50 m) FOR 16, 17, AND 18 MARCH 1970, AND 500 mb HEIGHT CONTOURS FROM NMC AT 0000 GMT FOR 17, 18, AND 19 MARCH 1970 (dashed lines at intervals of 6 decameters). (Grid-point analysis of cloud motion vectors superposed.)

GMT, while the constant-pressure contour analyses are valid at 0000 GMT. Since the mid-level cloud motions are unspecified as to absolute height, isolines of balanced height are labeled in relative units at intervals of 50 meters. The NMC height contours are labeled in absolute units at 60-meter intervals. The history of events in the NMC analyses is reflected in the cloud-motion analyses: The short-wave trough associated with the surface cyclogenesis over Texas on 16 March, the building high-pressure ridge over the eastern United States, and the trough development over the Rocky Mountains on 18 March are prominent features in the cloud-motion analyses. However, it is evident that the distribution of balanced height computed from the cloud-motion vectors compares best with the 700-mb NMC analysis, especially when contour gradients are considered. The gradients on the 500-mb maps exceed by far those of the cloud-motion analyses, i.e., the 500-mb wind speeds exceed the mid-level cloud-motion speeds.

Figures 7 and 8 suggest that the principal synoptic features are preserved when the fields of cloud-motion vectors are used to compute spatial distributions of balanced height. For this storm the mid-level assigned to the cloud motions appears closer to the 700-mb level than to 500 mb, which is compatible with the results of the vorticity analysis.

b. High Level

Figure 9 shows the spatial distribution of high-level cloud-motion vectors as determined from the display system for 17 March, and a photograph of the cloud structure illustrative of the series of 16 photographs from which the motion vectors were derived. The motion vectors south of 30°N are associated with subtropical jetstream cirrus. When measuring cloud velocities on the console, all cirrus-type clouds--including those south of 30°N over Mexico--were categorized as high level.

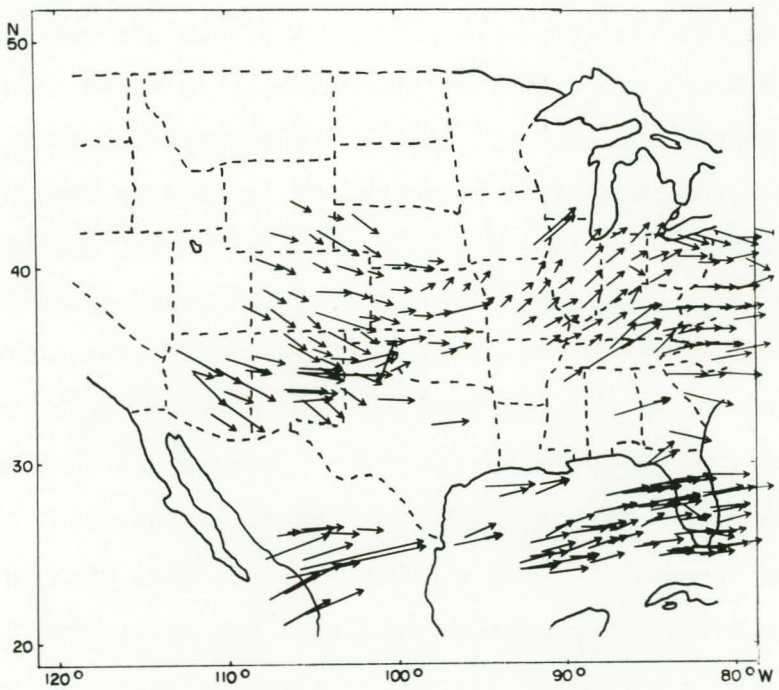

a) HIGH-LEVEL CLOUD MOTIONS

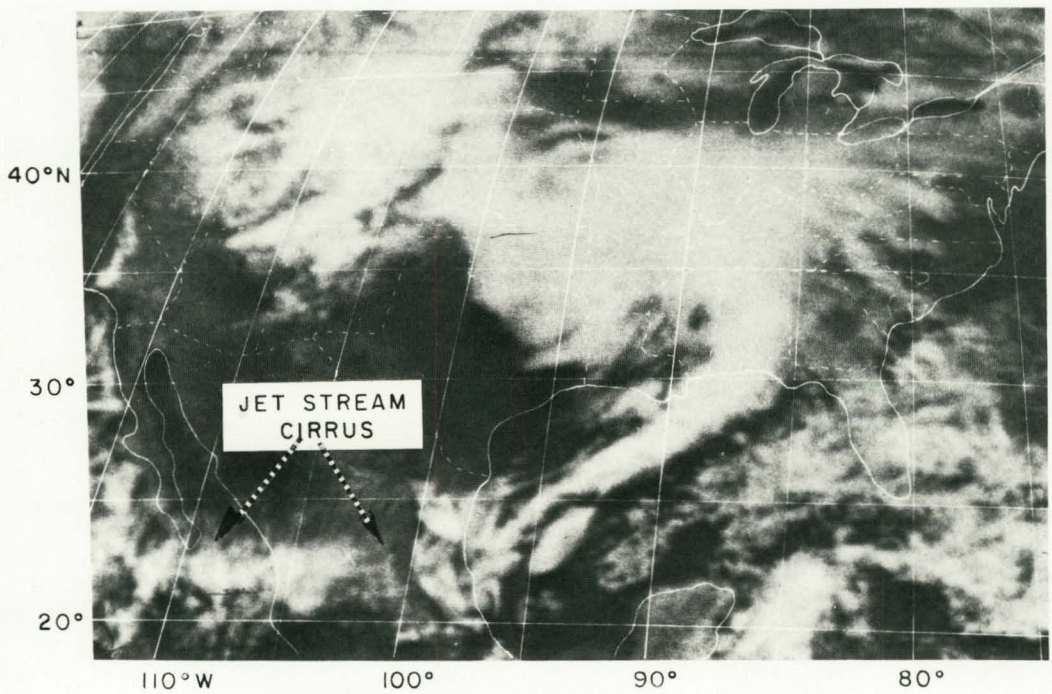

b) ATS PHOTOGRAPH, 2015GMT

FIGURE 9 SPATIAL DISTRIBUTION OF HIGH-LEVEL CLOUD MOTIONS AND ATS-III PHOTOGRAPH SHOWING ASSOCIATED CLOUD STRUCTURE FOR 17 MARCH 1970

The kinematic analyses of the high-level motion vectors of 17 March are evaluated by comparing computed patterns of balanced height and of relative vorticity with those obtained from concurrent rawinsonde data at various constant-pressure levels. In Figure 10, isolines of balanced height (in relative units at 50-meter intervals) computed from the high-level cloud motions of Figure 9 can be compared with those computed from rawinsonde data averaged for 1200 GMT 17 March and 0000 GMT 18 March at the 500-, 400-, and 300-mb levels. Over Mexico and the Gulf of Mexico the gradient of balanced height computed from the motion vectors is somewhere between that computed for the 400- and 300-mb levels. In the northern part of the analysis area, however (especially south of the Great Lakes), gradients of balanced height computed from the cloud motions are definitely less than those at the 400- and 300-mb levels, and correspond better to the 500-mb analysis. Thus, Figure 10 suggests that the high-level cloud velocities south of latitude 30°N probably correspond to a higher-level wind field than those over the continental United States north of 30°N.

Such a height difference is also suggested by the corresponding analyses of relative vorticity, which are shown in Figure 11. For example, Figure 11(a) shows an intrusion of relatively large cyclonic vorticity extending from north Texas into Kentucky. This feature reflects the pattern of large cyclonic vorticity centered around Arkansas and Missouri at the 500-mb level [Figure 11(b)]. South of 30°N, however, over southern Texas and northern Mexico, the cloud motion vectors do not have the anticyclonic vorticity of the wind fields at the 500-mb level, but rather the cyclonic vorticity analyzed from the horizontal wind field at the 400- and 300-mb levels [Figures 11(c) and (d)]. Thus, while the mid-level cloud motions show good correspondence to the 700-mb wind field, the analyses shown in Figures 10 and 11 demonstrate that the high-level cloud motions represent wind velocities at a combination of levels.

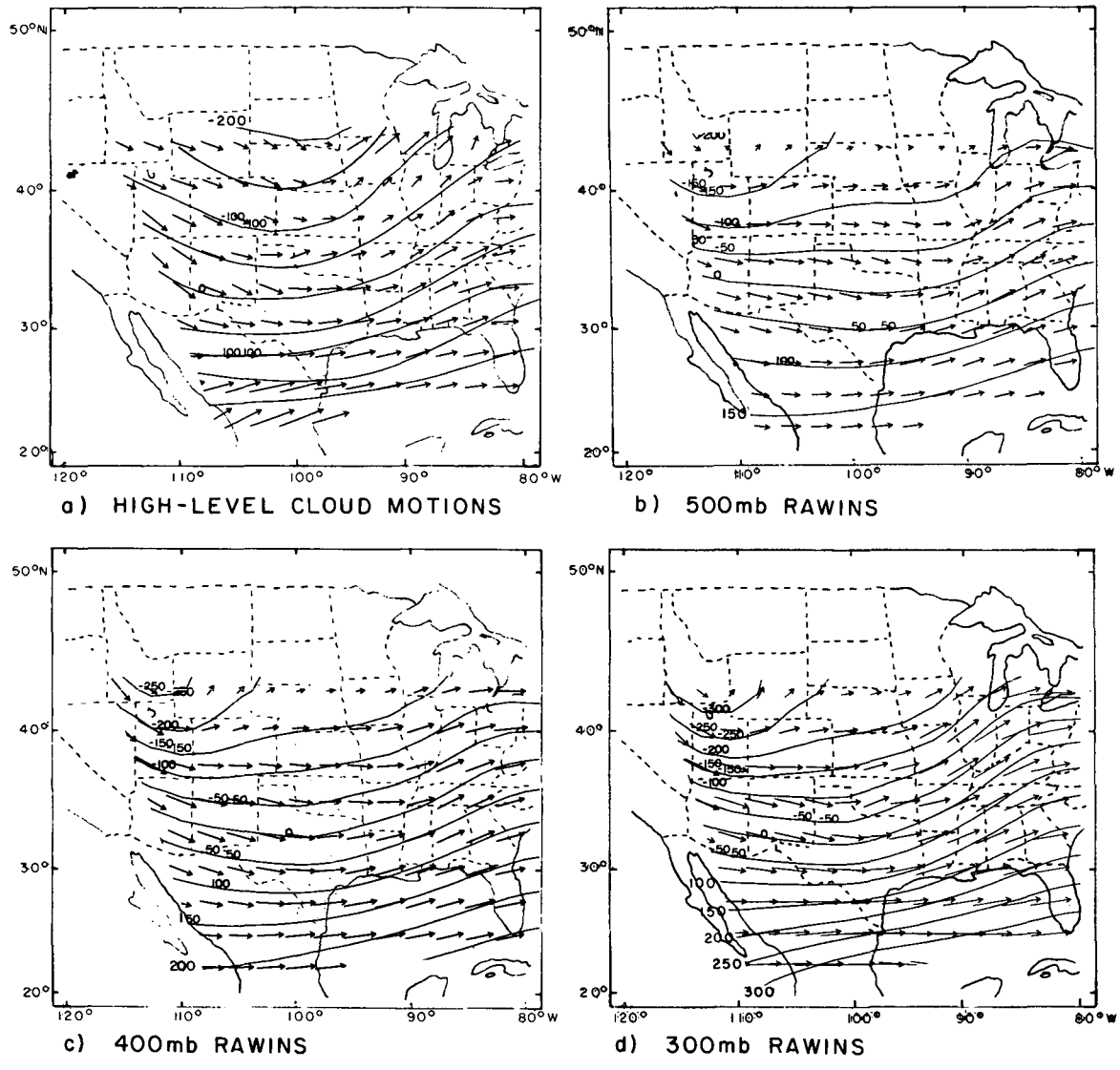

FIGURE 10 COMPARISON BETWEEN RELATIVE VARIATIONS OF BALANCED HEIGHT COMPUTED FROM HIGH-LEVEL CLOUD MOTIONS (a) AND FROM AVAILABLE RAWINSONDE DATA AT THREE CONSTANT-PRESSURE LEVELS (b), (c), AND (d) FOR 17 MARCH 1970. (Grid-point vector analyses superposed.)

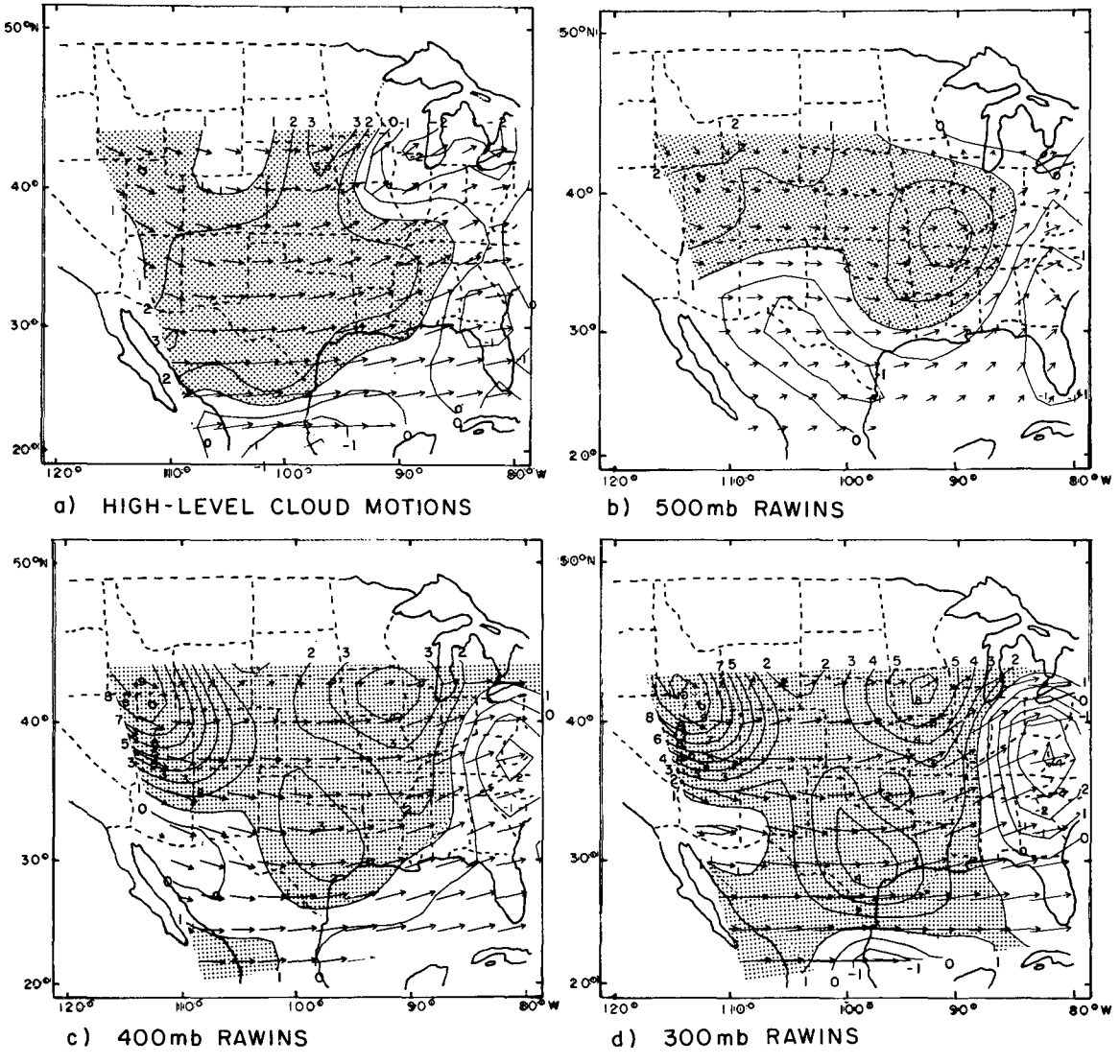

FIGURE 11 COMPARISON BETWEEN PATTERNS OF RELATIVE CYCLONIC VORTICITY (shaded; units: 10^{-5} sec^{-1}) COMPUTED FROM HIGH-LEVEL CLOUD MOTIONS (a) AND FROM AVAILABLE RAWINSONDE DATA FOR THREE CONSTANT-PRESSURE LEVELS (b), (c), and (d) FOR 17 MARCH 1970. (Rawinsonde data are averaged for 1200 GMT and 0000 GMT; Grid-point vector analysis superposed.)

Figure 12 shows scatter diagrams of grid-point values of vorticity computed from the high-level cloud motions of 17 March compared with values of vorticity computed at the same grid points from rawins. In Figure 12(a), the rawins refer to the 400-mb level; in Figure 12(b), they refer to the 700-mb level for grid points north of 30°N and to the 400-mb level for grid points south of 30°N. The combination of pressure levels gives a much improved correlation and linear fit. Thus, Figures 10 and 12 suggest that the high-level cloud motions represent wind velocities at a combination of levels.

The inability to assign the high-level cloud motions to a single level prevented useful interpretation of the kinematic analyses. The combination of levels to which the high-cloud motion analyses correspond is probably the result of a difference in height between the subtropical jetstream cirrus (south of 30°N over Mexico) and the cirrus-type clouds that were associated with the polar front cyclone and possibly with a polar jetstream. Normally the subtropical jetstream is at a higher level than the polar jetstream. Thus, when analyzing high-level cloud motions over an area that extends from a polar air mass into a subtropical air mass, polar frontal and subtropical cirrus cannot simply be categorized and analyzed together as "high level"; rather, accurate height discrimination as a function of latitude becomes important.

c. Absolute Values of Relative Vorticity

Table 3 lists the maximum values of relative vorticity that were computed from the mid-level and high-level cloud motions for each day. Also listed are maximum values of relative vorticity from the NMC analyses (daily averages from 1200 and 0000 GMT) and from the rawinsonde data averaged from 1200 GMT 17 March and 0000 GMT 18 March.

The vorticity values obtained from the cloud motions are reasonable as related to the stable frontal-wave type cyclone and to the

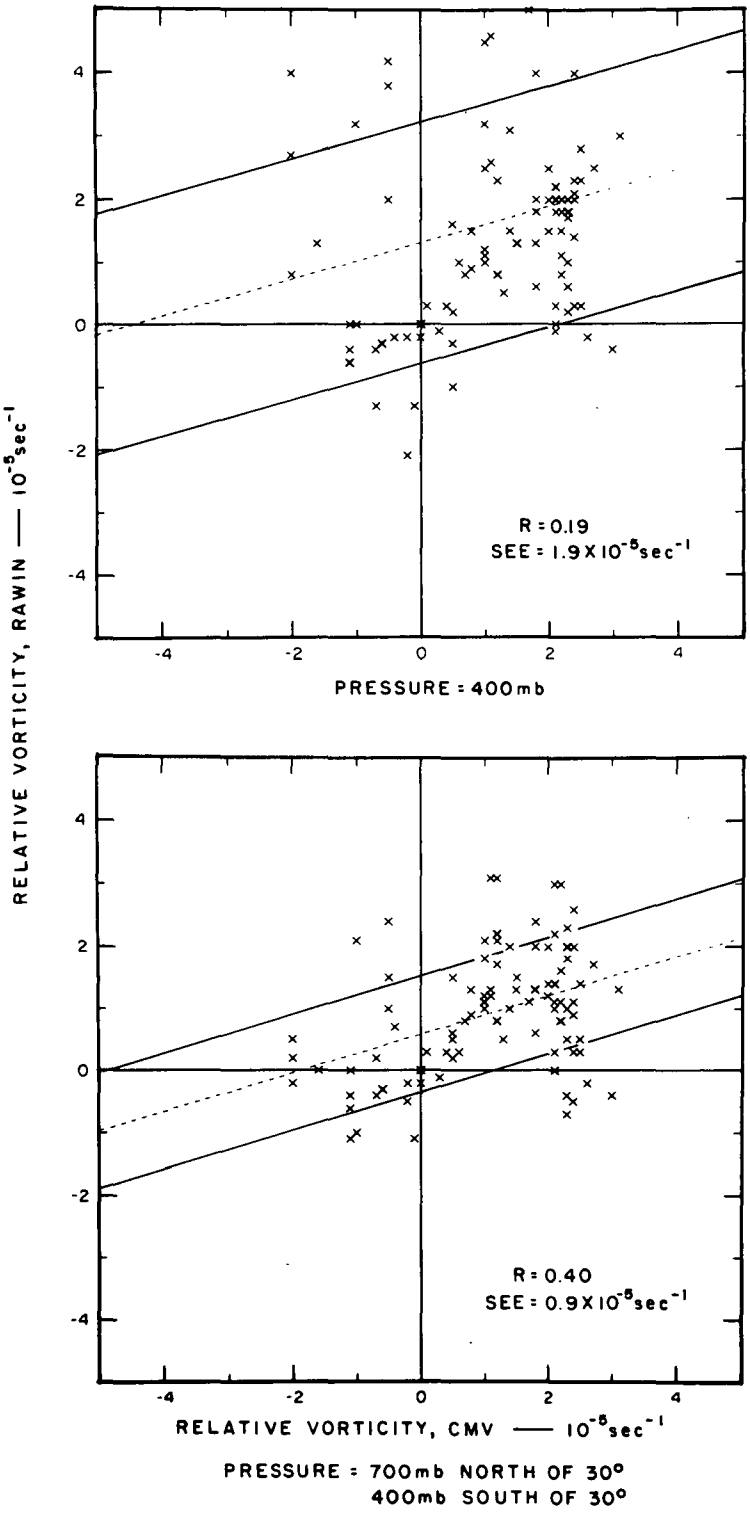

FIGURE 12 SCATTER DIAGRAMS SHOWING THE LINEAR REGRESSION OF RELATIVE VORTICITY COMPUTED FROM RAWINS (averaged for 1200 GMT and 0000 GMT) ON RELATIVE VORTICITY COMPUTED FROM HIGH-LEVEL CLOUD MOTIONS

Table 3

MAXIMUM VALUES OF RELATIVE VORTICITY
FROM CLOUD MOTIONS, NMC, AND RAWINS

Source	16 March		17 March		18 March	
	Cyclonic $10^{-5}s^{-1}$	Anticycl. $10^{-5}s^{-1}$	Cyclonic $10^{-5}s^{-1}$	Anticycl. $10^{-5}s^{-1}$	Cyclonic $10^{-5}s^{-1}$	Anticycl. $10^{-5}s^{-1}$
Mid-Level Cloud Motions	2.5	4.5	3.5	3.5	3.5	5.5
NMC	5.0	3.0	5.0	3.0	9.0	5.0
Rawins						
700 mb			3.5	1.5		
500 mb			3.5	1.5		
400 mb			4.5	2.5		
300 mb			6.5	4.5		

associated weak upper-level trough. Similar values were computed by Fujita et al. (1969) from the low-cloud velocities associated with a system of tropical storms. The values of Table 3, however, are smaller than those computed by Broderick (1969) for the 1000-500-mb layer (1×10^{-4} s^{-1}) and associated with a "Stage 2" cloud signature of the type shown in Figures 2, 3, and 4.

The tendency for larger NMC values, especially on 18 March, was evident from the scatter diagrams of Figure 5. The NMC analyses show maximum values of relative cyclonic vorticity ranging from 4 to 6 $\times$ 10^{-5} s^{-1} during the surface cyclogenesis east of the Rocky Mountains on 16 and 17 March, and from 8 to 10 $\times$ 10^{-5} s^{-1} during renewed cyclogenesis over the Rocky Mountains on 18 March. These values are about twice as large as those obtained from the cloud motions.

The increase of cyclonic vorticity with height indicated by the rawinsonde data on 17 March is not reflected by the values computed from the mid-level and high-level cloud motions. It is likely that the relatively small values associated with the high-level motions result from inadequate height discrimination. Also, the computer program develops a continuous field of vectors from the cloud motions obtained in areas where high-level clouds were identified. The interpolation and extrapolation technique used may reduce the large cyclonic shear and/or curvature that is frequently present near jet stream levels and near areas where high clouds are absent. In spite of the various discrepancies, we conclude that absolute values of relative vorticity computed from the cloud motion vectors for the period 16 to 18 March are acceptable.

D. Summary

This study has attempted to analyze and interpret patterns of relative vorticity and derived height computed from the cloud velocities associated with the cloud structure of an extratropical cyclone. Because

of the absence of data on the specific height of cloud elements measured, cloud motions were assigned to a mid-level (when subjectively classified as middle clouds), or to a high level (when subjectively classified as high clouds) on the basis of cloud appearance, and relative motion as observed on the SRI/NASA Electronic Display System.

Computations of relative vorticity using the mid-level cloud motion vectors showed encouraging results. Patterns of computed cyclonic vorticity related to the development, location, and movement of the surface cyclone. Computed values of relative vorticity showed good positive correlation with vorticity computed from concurrent rawinsonde data for the 700-mb level. The analyses of balanced height also suggest that the so-called mid-level corresponds better to the 700-mb level than to higher levels.

The vorticity analyses from the high-level motion vectors represented difficulties resulting from the wide latitudinal range in the height of cirrus. Cirrus-type clouds from both a polar jetstream and a subtropical jetstream were included in the high-level analysis. Not only is the subtropical jetstream normally at a higher level than the polar jetstream, but the banded cloud structure and sharp cloud edges that are frequently present near jetstream levels make it all but impossible to obtain representative values of relative vorticity from a field of motion vectors generated from individual cloud velocities.

Further research in computing relative vorticity from cloud motion vectors seems warranted, with particular emphasis on obtaining better height references. As a first step, for example, one might investigate the improvement obtained when the concept of the Level of Best Fit (LBF) is used to assign a probable height to a cloud-motion measurement and then limiting the altitude range of vorticity computations to or near this level. Also, computations should be made from cloud-motion measurements made over shorter time periods of ATS data than used in the present study.

With the ultimate addition of concurrent radiometric data, kinematic computations from cloud motions may yield quantitative information equal in value to that obtained from modeling techniques such as those investigated by McClain and Brodrick (1967). In data-sparse areas where satellite photographs show thick, multilayer cloudiness associated with cyclone development, computations of vorticity from cloud motions may supplement the information that eventually will be obtained from the vertical profiles of temperature supplied by spectral radiometric sounding techniques (SIRS), providing the needed input to numerical analysis and prediction.

III RELATIONSHIP OF CLOUD MOTION TO CHANGES IN CIRCULATION

The objective of this task was to ascertain whether there are any differences that occur between cloud motion and wind during a deepening pressure change or filling pressure change that would be useful in meteorological analyses. Selected samples of the cloud-motion vectors utilized in the computation of vorticity (Section II) were used. These vectors were treated in two ways:

- All vectors within 60 nmi of a rawin for the three-day period were analyzed to establish a background against which vectors associated only with the storm could be compared.
- Those vectors associated with the storm were analyzed with emphasis on 17 March, when the storm deepened slightly and on 18 March when the storm was filling.

These analyses necessitated a comparison with conventional winds as given by rawins.

Since the mid-time of the cloud-motion measurements was near 1800 GMT and the rawins are taken at 1200 and 0000 GMT, the rawins were time-adjusted to the time of the individual cloud-motion measurements. In the process, the computer generated an adjusted sounding (at 10-mb increments) that would have existed assuming the wind changed uniformly with time between the two soundings. The computer then compared the cloud-motion vector with this adjusted sounding and found the level of minimum vector difference between the cloud motion and the wind.

A. Analysis of All Cloud Motions within 60 nmi of a Rawin

1. Altitude of Level of Minimum Vector Difference

Figure 13 shows the frequency distribution of the levels of minimum vector difference, grouped by 50-mb increments. The number of occurrences spreads over a wide range from the 950-mb level to the 200-mb level. The figure shows a greater frequency of cases having low levels of best fit than with cases having high levels of best fit. Nearly 25 percent of the sample is in the interval 760 to 850 mb; a secondary concentration is found near the 400-mb level. This distribution is quite similar to that found by Serebreny et al. (1970a), who found modes at the 900-, 650-, and 350-mb levels in the analysis of clouds over the tropical and subtropical Atlantic and Pacific Oceans.

2. Differences between Cloud Motions and Winds at the Level of Minimum Vector Difference

Figure 14 shows the magnitude of the minimum vector difference for cloud motions with levels of minimum vector difference at various altitudes. The magnitude of the minimum vector difference ranges from 0 to 32 knots but generally does not exceed 25 knots except at or below the 850-mb level.

A summary of the differences between cloud motions and rawins at the level of best fit is given in Table 4, where the data are divided into two groups: those cases with a LMVD lower than the 500-mb level and those with a LMVD at or above the 500-mb level.

Cumulative frequency curves of direction difference, speed difference, and vector difference between the cloud-motion vector and the time-adjusted rawinsonde data were constructed and illustrated in Figure 15. The figure shows that less than 10 deg direction difference occurs in 56 percent of the measurements below the 500-mb level and in

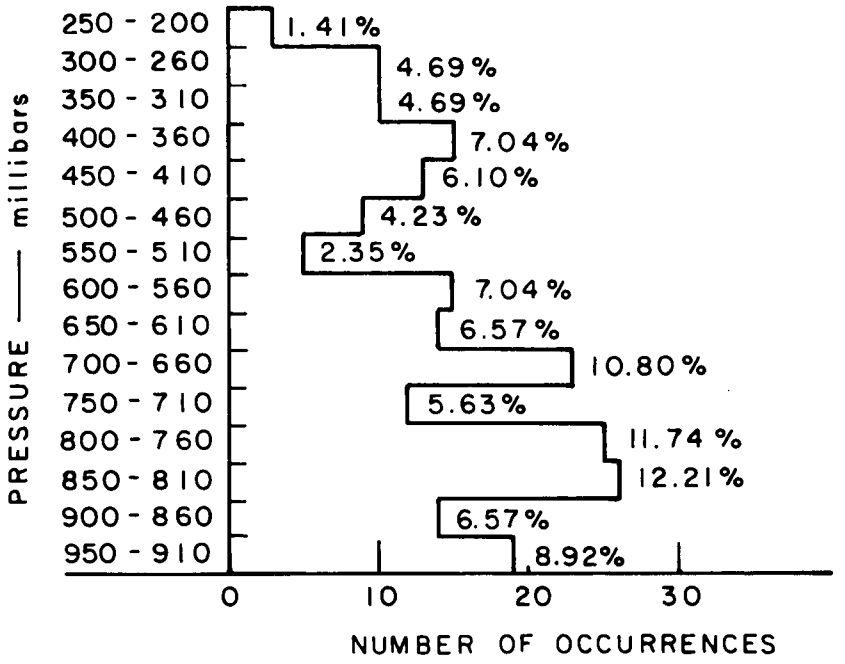

FIGURE 13 FREQUENCY DISTRIBUTION OF THE LEVELS OF MINIMUM VECTOR DIFFERENCE

Table 4

COMPARISON OF DIFFERENCES BETWEEN CLOUD MOTION AND WIND AT LEVEL OF MINIMUM VECTOR DIFFERENCE (LMVD)

Point of Comparison	LMVD	
	Below 500 mb	At or above 500 mb
Number of cases (N)	153	60
Mean direction difference (degrees)	12.6	6.9
Mean speed difference (knots)	5.1	3.4
Mean magnitude of vector difference (knots)	7.9	7.1
σV^* (knots)	10.3	9.2

*Standard vector deviation = $\sigma V = \sqrt{\frac{\Sigma_i^N R_i^2}{N}}$ where R_i = vector difference, N = number of cases.

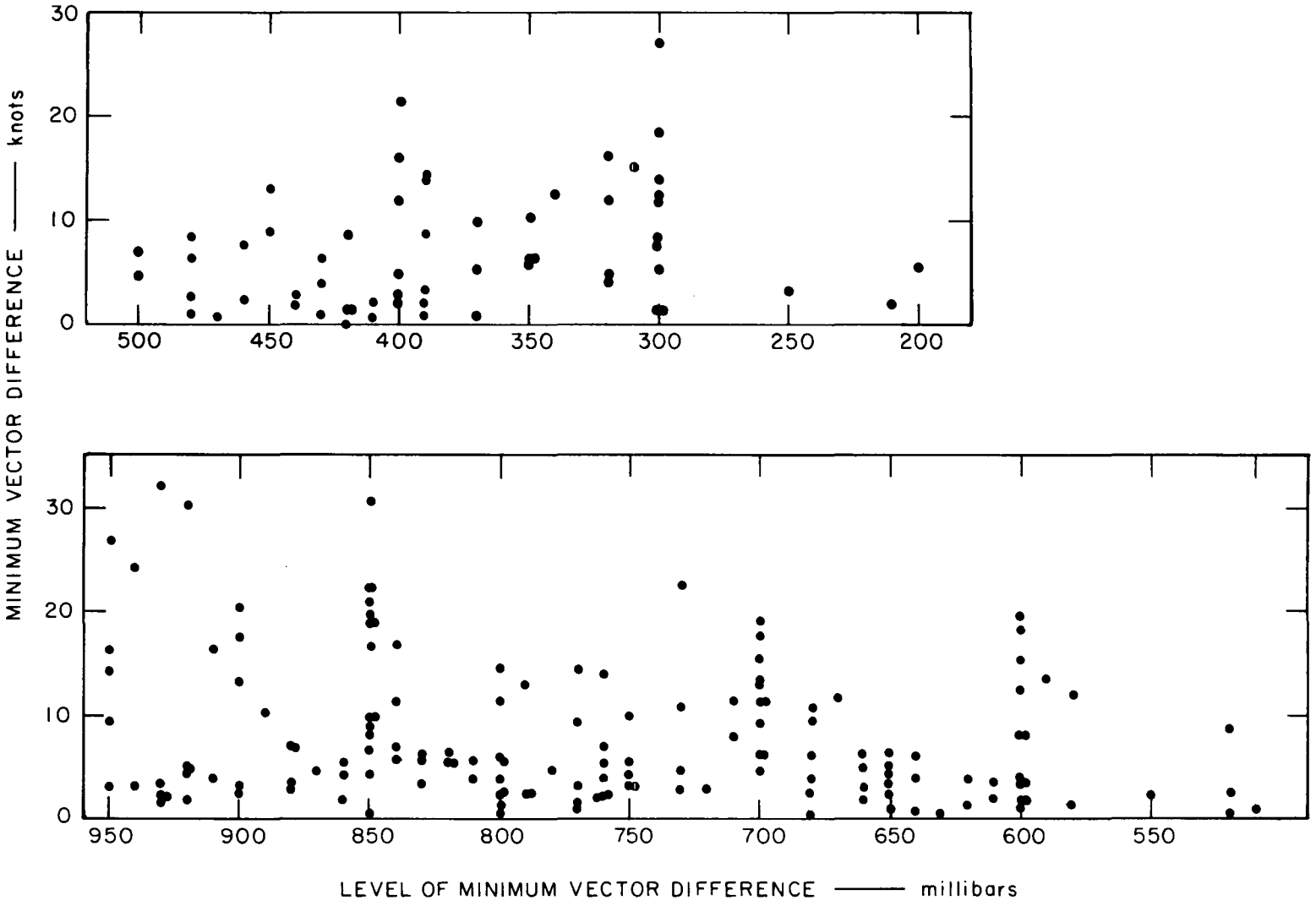

FIGURE 14 MAGNITUDE OF MINIMUM VECTOR DIFFERENCE VERSUS LEVEL OF MINIMUM VECTOR DIFFERENCE

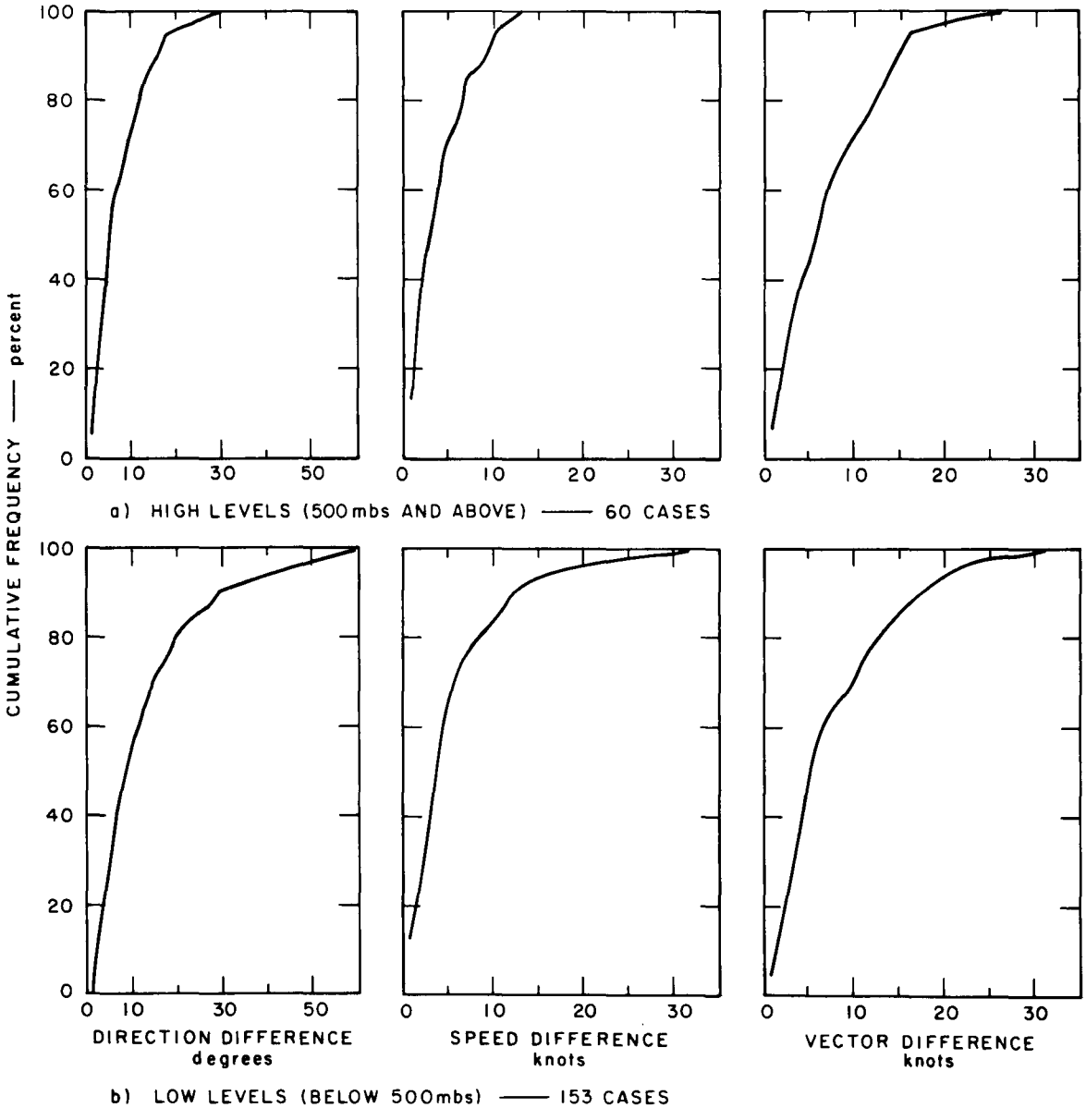

FIGURE 15 CUMULATIVE FREQUENCIES OF DIRECTION, SPEED, AND VECTOR DIFFERENCES BETWEEN CLOUD MOTION VECTORS AND WINDS AT THE LEVEL OF BEST FIT

73 percent of the measurements at levels above. Less than 10 knots speed difference occurs in 84 percent of the measurements below the 500-mb level and in 95 percent above. Less than 10 knots minimum vector difference occurs in 71 percent of measurements below the 500-mb level and in 72 percent of the measurements above.

3. Effects of Assigning Cloud Motions to Levels Other than the Level of Best Fit

The contract called for a determination of the vector difference between the cloud motion and the wind at the 850-mb level for low clouds and the wind at the 300-mb level for high clouds. Accordingly, cloud motions with LBFs below the 500-mb level were compared with winds at the 850-mb level and those with LBFs at or above the 500-mb level were compared with 300-mb level winds.

Figure 16 shows the scatter diagrams resulting from this comparison. The figure shows that the 300-mb wind speeds were generally larger than cloud speeds (for clouds with LMVDs at or above the 500-mb level). The comparison between 300-mb wind direction and cloud direction (for clouds with LMVDs at or above the 500-mb level) shows most of the points clustering around the one-to-one line, while the largest deviations show the clouds moving to the right of the 300-mb wind direction. The clouds with LMVDs below the 500-mb level are divided into two groups on Figure 16: those with LMVDs from 699 to 501 mb and those with LMVDs at or below the 700-mb level. Comparison of these two groups with the 850-mb wind speed shows that the higher group tends to have speeds larger than the 850-mb wind speed, while the lower group is approximately bisected by the one-to-one line. With respect to direction, the cloud motions in the group 699 to 501 mb tend more to move to the right of the wind than the lower group does. The lower group is about evenly scattered either side of the one-to-one line.

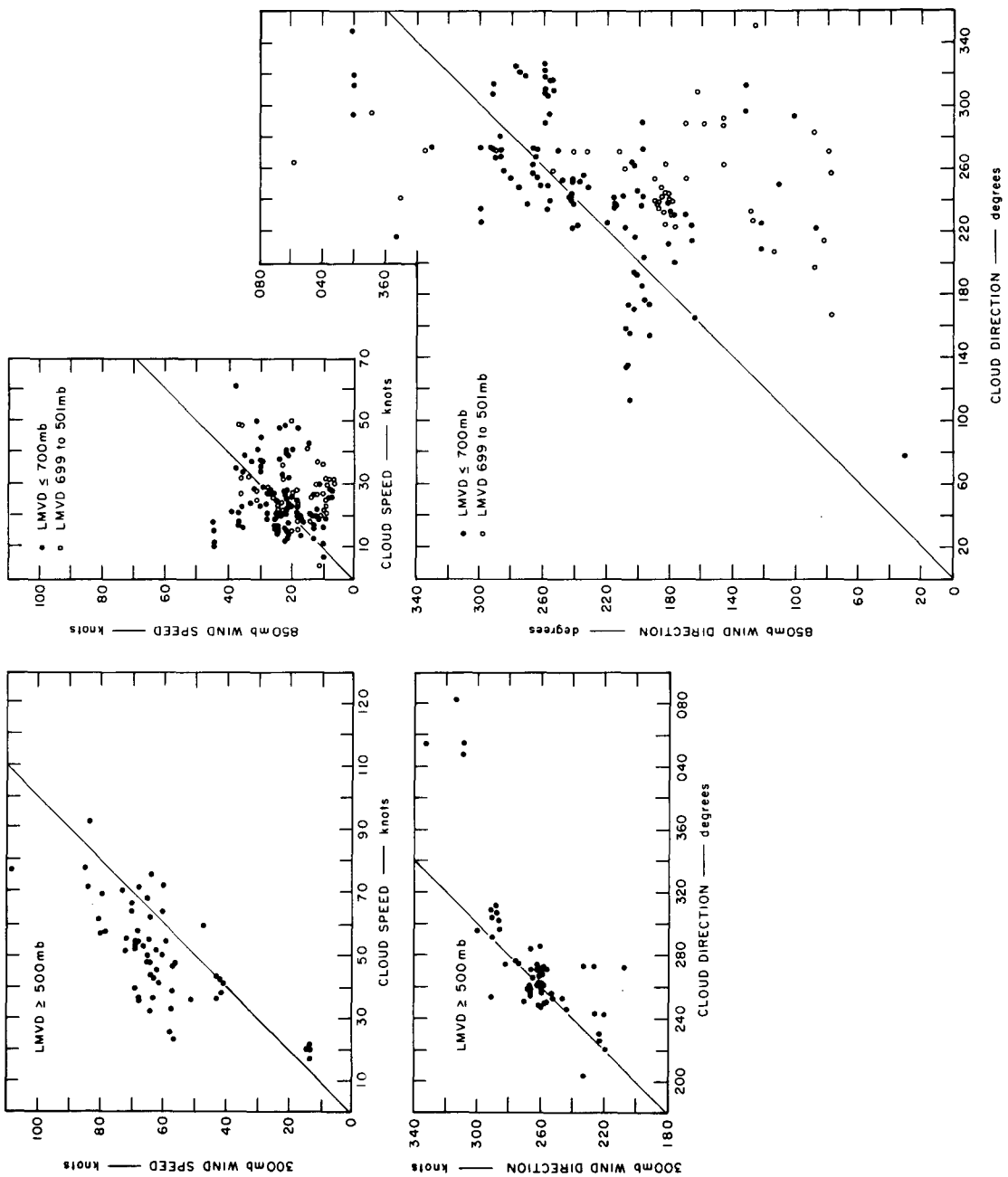

FIGURE 16 COMPARISON OF CLOUD DIRECTION AND SPEED WITH WIND DIRECTION AND SPEED

Figure 17 shows the resulting vector differences when the minimum vector difference was subtracted from the vector difference at the 300-mb level for higher clouds and from that at the 850-mb level for lower clouds. The figure demonstrates quite clearly the limitation of assigning winds from a number of diverse levels to any level significantly different from the original level. For example, while vector differences at the level of minimum vector difference showed few cases with values in excess of 25 knots (Figure 14) Figure 17 shows a number of cases with values in excess of 30 knots. The magnitude of the difference increases with increasing departure from the 850- and 300-mb levels (where, by definition, it is zero). The reason for the increases are undoubtedly due in large part to vertical wind shear.

To ascertain just how much manipulation of the winds from one level to another could possibly be justified or considered practical we chose to examine further the effects of limited displacement of winds within each of three selected pressure intervals. The intervals we chose were 850-750, 650-550, and 450-350 mb. The cumulative frequency of vector differences within these layers was then compared to the cumulative frequency of averaged vector differences at plus and minus 50, 100, and 150 mb from the LMVD. The results are shown in Figure 18. (Note: to expand the data sample, cloud measurements on 15 March are included as well as those on 16, 17, and 18 March.)

Table 5 summarizes the percentage of cases with vector differences 10 knots or less within each layer and for each displacement.

These comparisons would discourage the assignment of winds derived from cloud-motion measurements to any level $\geq$ 50 mb from the LMVD or from any cloud altitude determined by radiometric information.

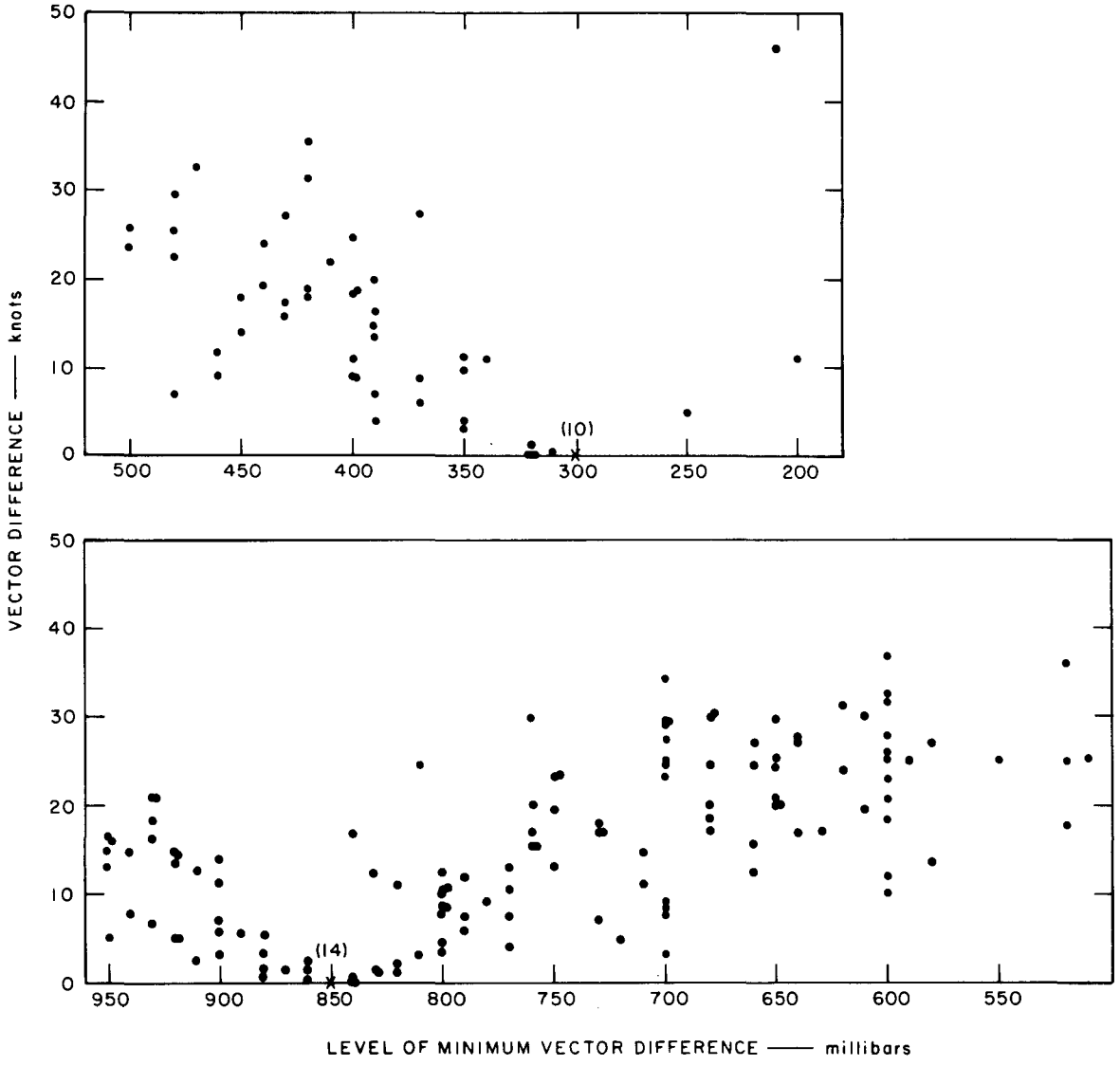

FIGURE 17 RESULTING VECTOR DIFFERENCE WHEN MINIMUM VECTOR DIFFERENCE IS SUBTRACTED FROM 300-mb VECTOR DIFFERENCE FOR CLOUD MOTIONS WITH LBFs AT OR ABOVE THE 500-mb LEVEL OR FROM 850-mb VECTOR DIFFERENCE FOR CLOUD MOTIONS WITH LBFs BELOW THE 500-mb LEVEL

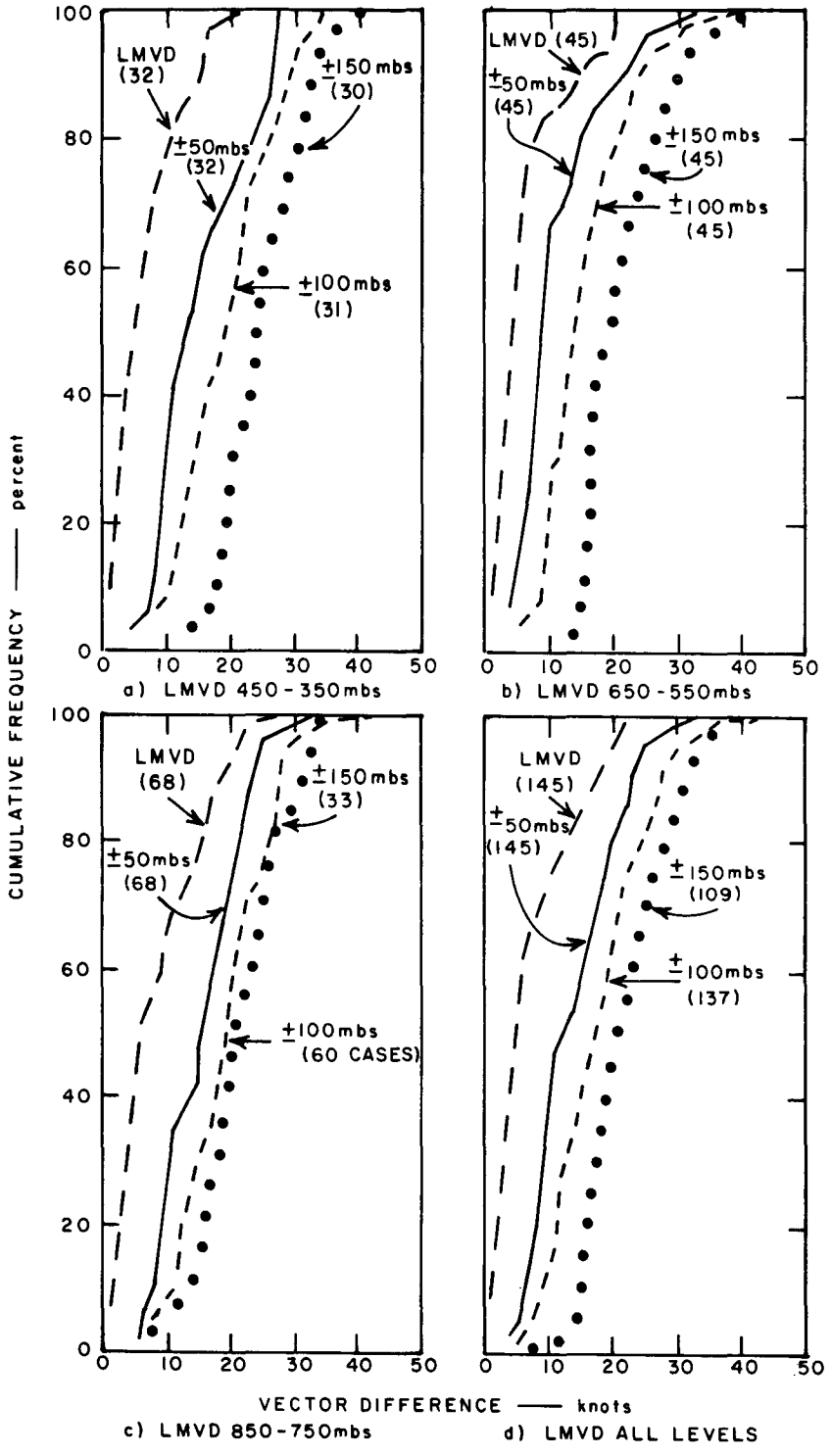

FIGURE 18 COMPARISON OF CUMULATIVE FREQUENCIES OF VECTOR DIFFERENCES AT LEVEL OF BEST FIT WITH CUMULATIVE FREQUENCIES OF VECTOR DIFFERENCES ± 50, ± 100, AND ± 150 mbs FROM LEVEL OF BEST FIT FOR THREE ALTITUDE RANGES

Table 5

COMPARISON BETWEEN PERCENTAGE OF CASES WITH VECTOR DIFFERENCE ≥ 10 KNOTS AT LMVD AND PRECENTAGE OF CASES WITH VECTOR DIFFERENCE ≥ 10 KNOTS WHEN CLOUD MOTIONS IN SELECTED LAYERS ARE DISPLACED ± 50, ± 100, and ± 150 MBS FROM LMVD

Layer (mb)	Percentage of Cases			
	At LMVD	± 50 mb	± 100 mb	± 150 mb
850-750	66	28	9	6
650-550	84	66	28	0
450-350	78	21	10	0

B. Analysis of Cloud Motion Vectors Associated with Storm

Figures 19, 20, and 21 show the storm on 16, 17, and 18 March, respectively. An overlay to each cloud photograph shows the frontal positions, locations of measured clouds associated with the storm, heights in tens of millibars, and contours of the level of best fit between cloud motion and rawin data within 60 nmi of the measured cloud. Examination of the level of best fit on 16 March (Figure 19) shows values below the 900-mb level near the center of the cloud shield while values around the edges are at or above the 700-mb level. Vertical profiles of relative humidity, as shown by radiosonde data, were examined to determine whether the clouds were actually lower near the center of the shield, rather than at the edges. This examination showed high values of relative humidity to considerably higher levels than the computed level of best fit. For example, at one station where levels of best fit for three measured clouds were 830, 800, and 780 mb, the humidity was in excess of 90 percent up to the 600-mb level. In such instances, the

20

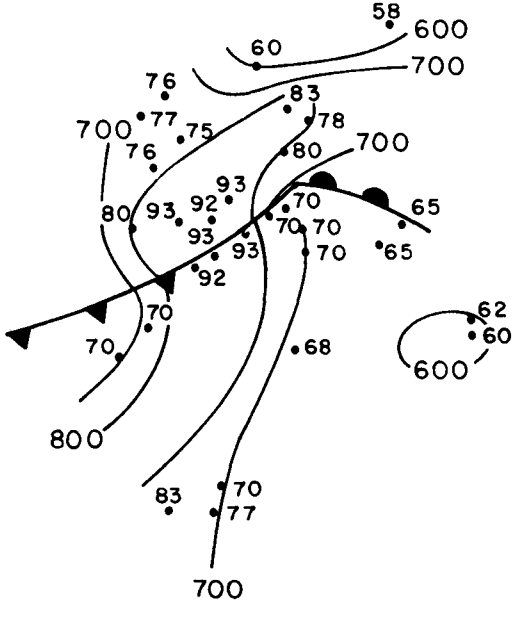

FIGURE 19 CLOUD COVER AND LEVEL OF BEST FIT ON 16 MARCH 1970

OVERLAY FOR PAGE 50

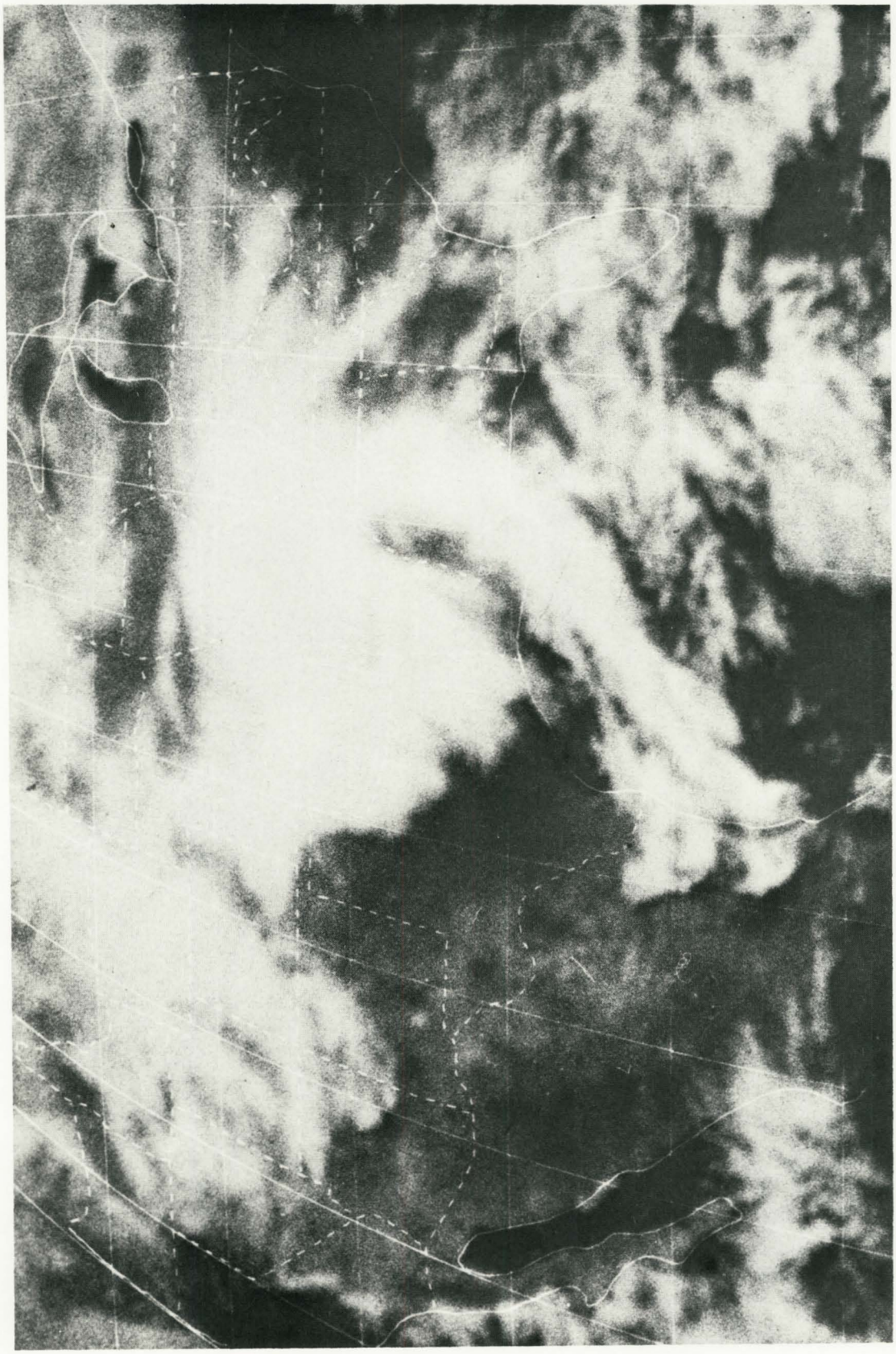

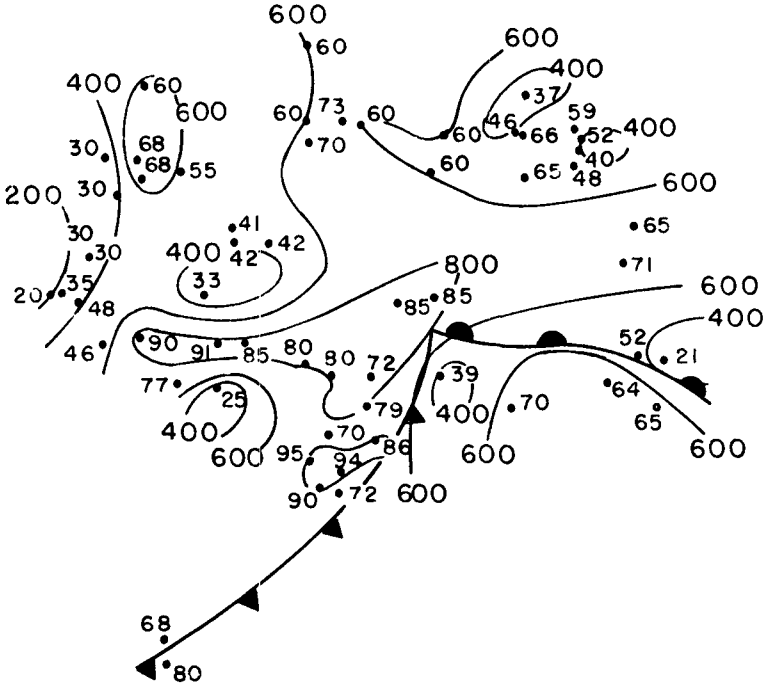

FIGURE 20 CLOUD COVER AND LEVEL OF BEST FIT ON 17 MARCH 1970

OVERLAY FOR PAGE 51

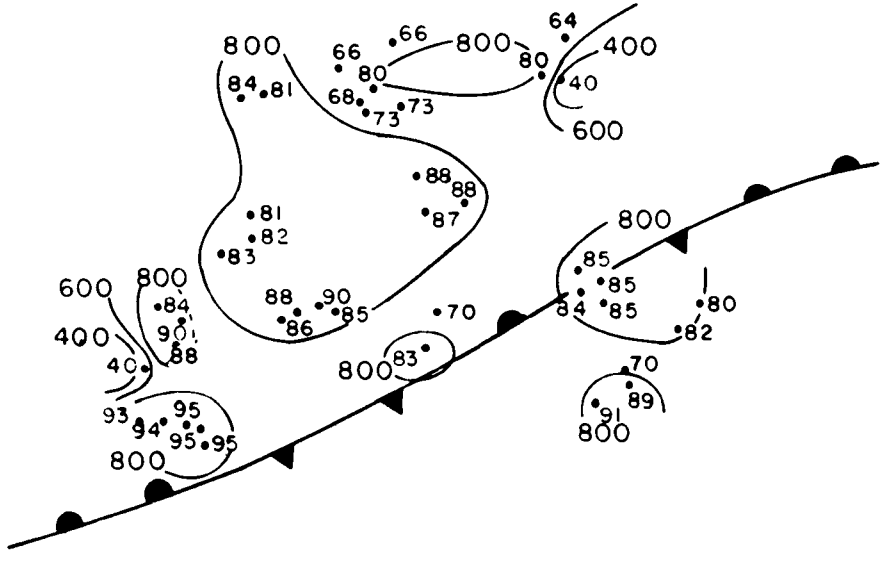

FIGURE 21 CLOUD COVER AND LEVEL OF BEST FIT ON 18 MARCH 1970

OVERLAY FOR PAGE 52

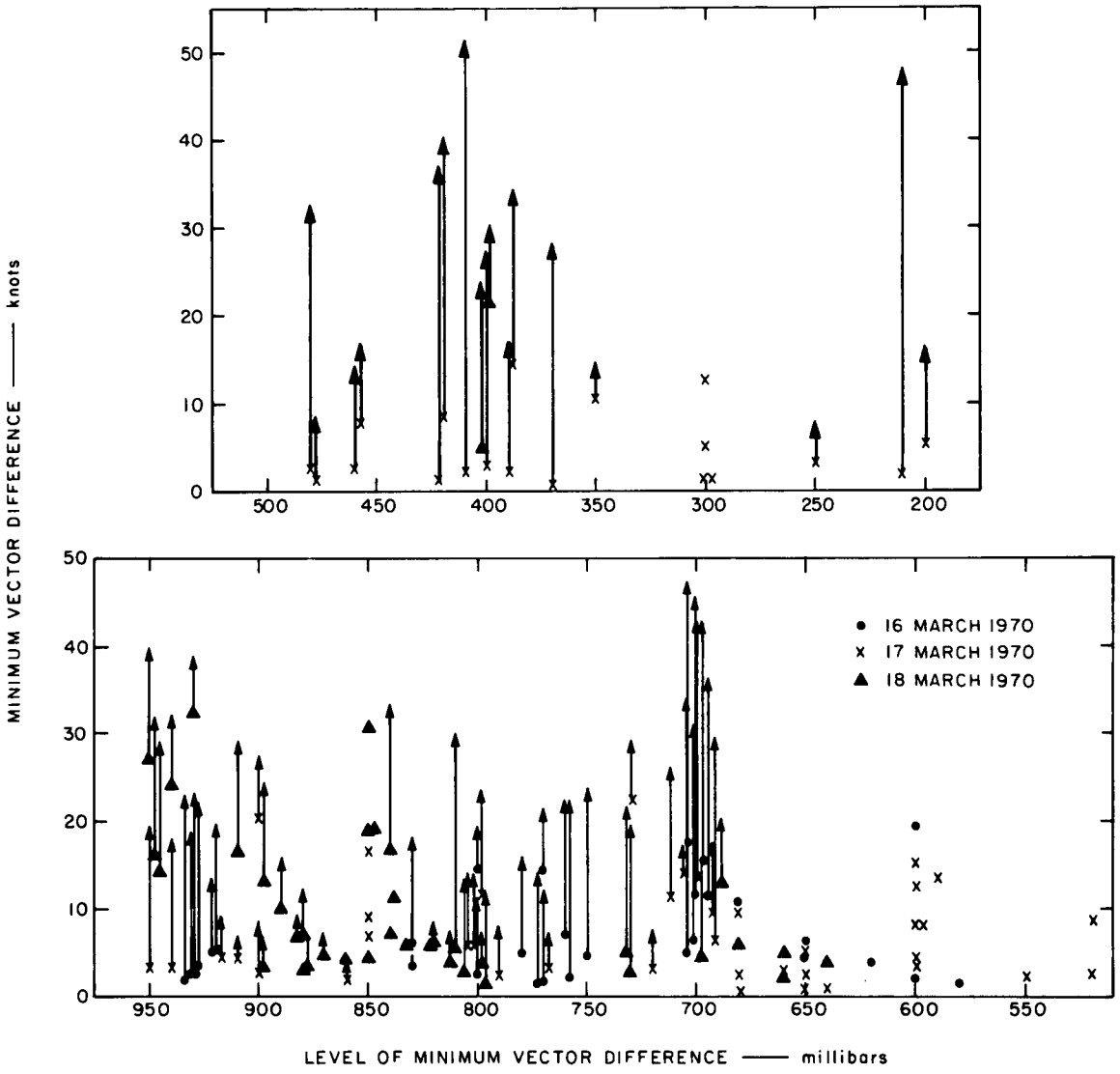

FIGURE 22 MINIMUM VECTOR DIFFERENCE AT THE LEVEL OF MINIMUM VECTOR DIFFERENCE (LMVD) AND THE CHANGE IN MINIMUM VECTOR DIFFERENCE WHEN CLOUD MOTIONS WITH LMVD AT OR ABOVE THE 500-mb LEVEL ARE COMPARED WITH 300-mb WINDS AND CLOUDS WITH LMVD AT OR BELOW THE 700-mb LEVEL ARE COMPARED WITH 850-mb WINDS (clouds between the 700- and 500-mb levels were not compared with upper or lower level winds)

featureless stratiform nature of the cloud cover apparently makes it impossible to measure the cloud motion accurately.

On 17 March (Figure 20), the level of best fit is lowest over Arkansas and northeast Texas (well within the cloud mass) and higher values are generally found around the edges. The highest value was over northern Texas, where a point at the 200-mb level was computed. Again the low levels of best fit are undoubtedly due to the difficulty of finding a well-defined cloud feature to follow. In fact there are some large areas with no data points showing that it was impossible to make measurements.

On 18 March (Figure 21), levels of best fit were below the 800-mb level over nearly the entire area. The only exceptions are over Ohio and east Texas, where levels as high as the 400-mb level were computed. Radiosonde ascents over the area at this time showed the top of the layer of high humidity extending only to rather low levels--generally well below the 800-mb level; hence much of the cloud is probably low. Much of the cloud, for example, over southeastern United States has features that could be tracked so the measurements would be more accurate than those taken within a featureless cloud cover.

Figure 22 shows the distribution by pressure level of the levels of minimum vector difference between winds and cloud motion measurements associated with the storm system for the three days. Also shown is the magnitude of the minimum vector difference and the change in vector difference when cloud motions at or below the 700-mb level were compared with winds at the 850-mb level and when cloud motions at or above the 500-mb level were compared with 300-mb level winds. Levels of minimum vector difference and magnitudes of minimum vector difference on this figure show essentially the same variability as Figure 14, which contained measurements not associated with the storm as well as those associated with the storm. The length of the arrows on Figure 22 shows the

change in vector difference when cloud motions with levels of minimum vector difference at or above the 500-mb level are compared with 300-mb winds and when cloud motions with levels of minimum vector difference at or below the 700-mb level are compared with 850-mb winds (clouds between 700 and 500 mb were not used for comparison with low- or high-level winds). The changes in minimum vector difference when these comparisons are made increase substantially for the upper-level clouds. The changes are not as great for the lowest clouds but are quite large for those with a level of minimum vector difference near the 700-mb level. For both the lower- and upper-level clouds, the changes in minimum vector difference are very similar to those shown by Figure 17 where all clouds during the three-day period were considered.

Figure 23 shows cumulative frequency curves of direction, speed, and vector differences between cloud motion vectors and winds at the level of minimum vector difference for clouds associated with the storm. The data are divided into two groups: those cases with LMVD at or above the 500-mb level and those cases with LMVD below the 500-mb level. The figure shows that upper-level direction differences are smaller than low-level direction differences. The same is true also of speed differences and therefore, vector differences.

Table 6 compares differences shown by Figure 23 with those shown by Figure 15 (which included all measurements on the three days). Table 6 shows similar values for clouds with LMVD below the 500-mb level. At the upper levels, the percent of clouds having a direction difference less than 10 deg was much higher for the storm than for the three-day sample. Not as great a percentage of cases associated with the storm had speed differences less than 10 knots. The percent of cases with a vector difference less than 10 knots is greater for the storm only than for the three-day sample.

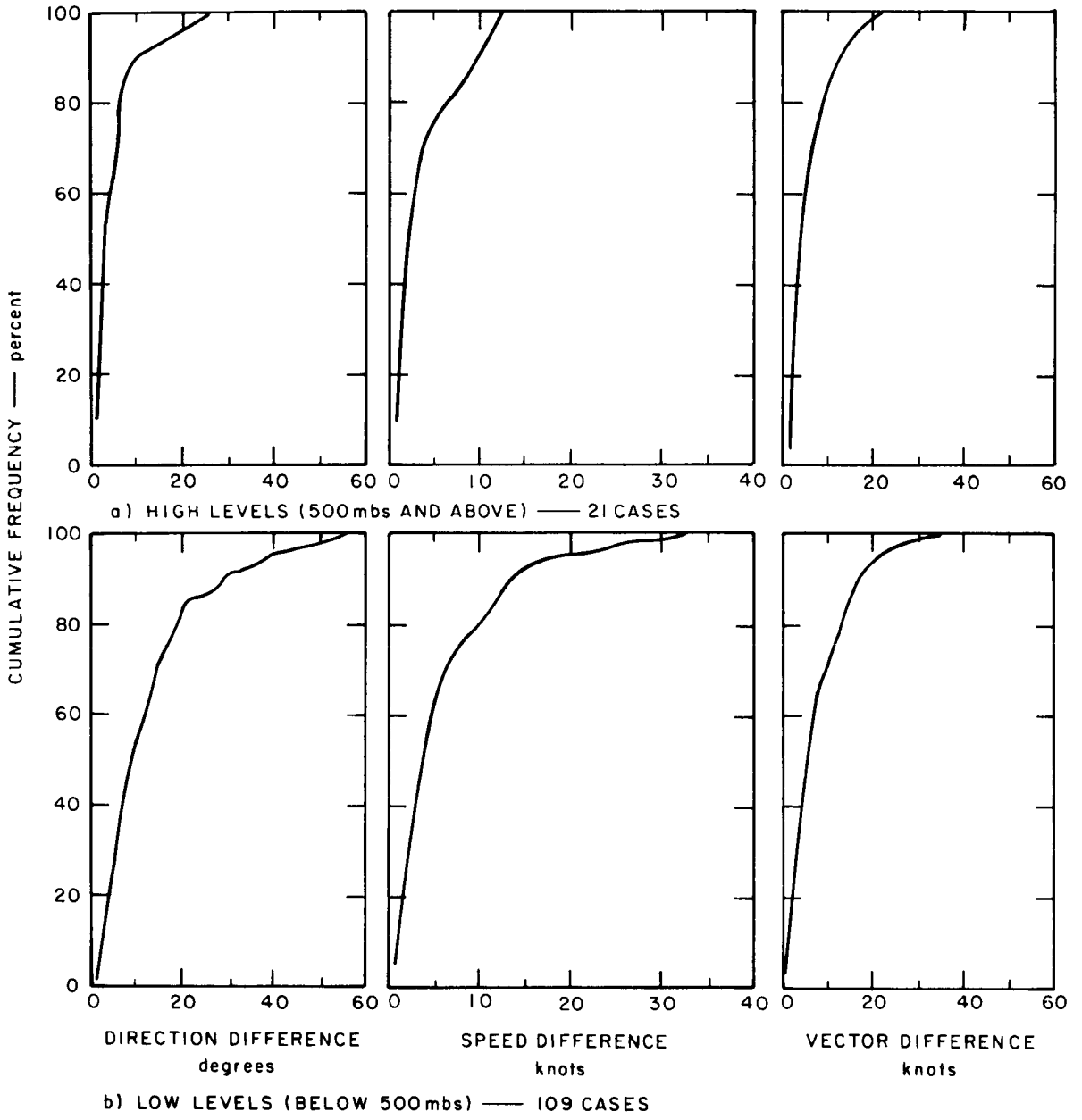

FIGURE 23 CUMULATIVE FREQUENCIES OF DIRECTION, SPEED, AND VECTOR DIFFERENCE BETWEEN CLOUD MOTION VECTORS AND WINDS AT THE LEVEL OF BEST FIT

Table 6

COMPARISON BETWEEN ALL MEASUREMENTS DURING THE THREE-DAY PERIOD AND THOSE ASSOCIATED WITH THE STORM

Basis of Comparison	LMVD	
	Below 500 mb	At or above 500 mb
Number of cases		
Three days	153	60
Storm only	109	21
Direction difference < 10 deg		
Three days	56%	73%
Storm only	55%	90%
Speed difference ≤ 10 knots		
Three days	84%	95%
Storm only	80%	90%
Vector difference < 10 knots		
Three days	71%	72%
Storm only	70%	83%

Data for all measurements for the three-day period were summarized for comparison with data for the storm system when it was deepening (17 March) and filling (18 March). Table 7 shows the results of this comparison. The major differences shown by the table are that on 18 March there was an absence of measurable high clouds; only two cases compared with 19 on 17 March. The average cloud speed both at low and high levels was faster on 18 March than on 17 March. The speed on 17 March was close to the three-day average. The average direction difference between the cloud-motion vector and wind at the level of best fit was smaller for low-level clouds on 18 March than on 17 March but was larger for clouds with LMVD ≥ 500 mb in the two cases available. The average speed difference between cloud motion and wind at the level of minimum vector difference was greater on 18 March than on 17 March and

Table 7

COMPARISON OF ALL MEASUREMENTS DURING ALL THREE DAYS WITH THOSE ASSOCIATED WITH THE STORM ONLY DURING DEEPENING (17 MARCH) AND FILLING (18 MARCH) STAGES

Basis of Comparison	LMVD ≤500 mb	LMVD ≤700 mb	LMVD ≤700 Compared to 850 mb	LMVD ≥500 mb	LMVD ≥500 Compared to 300 mb
Number of cases					
17 March	39	21	21	19	19
18 March	39	35	35	2	2
3 days	153	108	104	60	60
Average cloud speed (knots)					
17 March	26.3	25.4		46.9	
18 March	29.9	30.5		63.0	
3 days	25.8	25.0		50.1	
Average direction difference (deg)					
17 March	12.4	12.6	30.2	4.0	15.3
18 March	11.4	11.6	30.5	11.0	16.0
3 days	12.6	13.5	41.4	6.9	17.5
Average speed difference					
17 March	4.1	4.9	7.0	3.1	14.7
18 March	7.4	8.2	10.3	6.5	16.0
3 days	5.1	6.1	9.6	3.4	13.7
Average vector difference					
17 March	7.0	8.0	15.3	4.7	22.5
18 March	9.6	10.2	16.7	13.4	27.2
3 days	7.9	8.8	18.8	7.1	20.6
Standard vector deviation					
17 March	8.9	10.0	17.3	6.2	26.5
18 March	12.6	13.2	20.1	15.7	27.3
3 days	10.3	11.3	21.6	9.2	23.1

this together with the larger direction difference causes the average vector difference to also be larger. The standard vector deviation is also larger.

When cloud motions with LMVD $\leq$ 700 mb were compared to the 850-mb winds, there was essentially no difference between the average direction difference on 17 March and 18 March; both days had values less than the three-day average. The average speed difference on 18 March was higher than on 17 March, but not significantly different from the three-day average. The average vector difference is greater on 18 March than on 17 March, but not as large as for the three-day average. The standard vector deviation shows the same trend as the average vector difference.

No valid comparison can be made of the three data samples when cloud motions with LMVD $\geq$ 500 mb are compared with 300-mb winds because of only two cases on 18 March. All averages, however, increase considerably over those at the LMVD.

These comparisons show that the basic difference in cloud motions between the deepening and filling stages are that during the filling stage most of the clouds were lower, moved faster, departed less from the wind direction but showed larger variation from the wind speed resulting in a greater average vector difference and larger standard vector deviation.

C. Summary

Comparison of cloud motion measurements on 16, 17, and 18 March 1970 showed that 150 of the 213 measurements agreed best with winds below the 500-mb level.

Investigation of differences between cloud motions and winds at the level of best fit was made for clouds with LBFs below and at or above the 500-mb level. The mean direction difference for the two groups was

12.6 and 6.9 deg; the mean speed difference 5.1 and 3.4 knots; the mean magnitude of vector difference 7.9 and 7.1 knots; and the standard vector deviation 10.3 and 9.2 knots.

The effect of assigning clouds to levels other than the level of best fit was examined. Clouds with a LBF $<$ 500 mb were compared with 850-mb winds and clouds with a LBF $\geq$ 500 were compared with 300-mb winds. These comparisons showed a considerable increase in the magnitude of the vector difference. A further study where cloud motions were compared with winds ±50, ±100, and ±150 mb from the level of best fit showed that the smaller interval (±50 mb) was the maximum amount that measured cloud motions could be moved from the level of best fit without introducing substantial errors.

Examination of only those cloud vectors associated with a cyclone was made and statistics during deepening compared with those during filling. The basic difference between the two stages was that there were very few high clouds during the filling stage; the cloud speeds were high and the cloud motions departed less from the wind direction, but showed larger variation from the wind speed. This resulted in a larger average vector difference and larger standard vector deviation during filling than during deepening. The differences in this case, however, where only slight deepening and filling occurred are not considered significant enough to be applied to any storm shown by ATS photographs to determine whether it is deepening or filling.

IV RELATIONSHIP OF CLOUD MOTION TO CLOUD SIZE

The objective of this task was to develop, if possible, correlations between cloud motion and conventional wind in tropical latitudes and to determine how correlation varies as a function of individual cloud size, cluster size, magnitude of wind vector, and weather type. Data for this task consisted of ATS photographs and rawins collected by stations in the BOMEX network.

A. Cloud Cover and Measurements

ATS photographs over the Caribbean were examined to find cases with data suitable for analysis during the period of BOMEX. During this period there were many days on which the pictures contained noise and scan line dropouts making them difficult or impossible to analyze. Four dates were found, however, on which the noise was within tolerable limits. The dates and the number of cloud measurements on each date are listed in Table 8.

Table 8

NUMBER OF CLOUD MEASUREMENTS
ON VARIOUS DATES

Date	Number of Measurements
12 July 1969	28
13 July 1969	31
26 July 1969	33
27 July 1969	38

The measurements were made in such a manner that, in addition to cloud direction and speed, the average cloud size, orientation of major and minor axes, and rate of change of cloud size could be computed.

Figures 24 to 27 show cloud cover as viewed by the ATS satellite and the size, shape, and velocity vector of measured clouds. Since cloud elements were forming and dissipating over short periods and measurements were made from photographs taken over a period of a few hours, an illustrated vector may be related to a cloud that does not appear in the illustrated photograph but was present on some of the other photographs in the sequence.

Examination of the cloud photographs and the measured clouds shows that on 12 July (Figure 24) most of the clouds north of the 10th parallel were small; nearly all were moving from an easterly direction. The 1200 GMT NMC Tropical Strip Surface Chart for this date showed the intertropical convergence zone extending east-west along 7°N corresponding to the more extensive cloud cover along the coast of South America.

On 13 July (Figure 25), the cloud patterns over the area remain similar to that of 12 July. Again all the clouds were generally moving from an easterly direction. The 1200 GMT surface chart showed the intertropical convergence zone extending east-west along 10°N, which is just north of the extensive cloud cover on the lower part of Figure 25(a).

On 26 July (Figure 26), there is a large cloud mass near the center of the cloud photograph with small clouds over most of the remainder of the area. Motions of clouds over the area do not show the generally uniform easterly motion of the previous two days illustrated; some motions are from the north while others have a strong southerly component. There was no surface chart for 1200 GMT on 26 July, but the 0000 GMT chart for 27 July showed a closed low (labeled a Tropical Depression) located at 16°N 61°W. This position is just west of the cloud mass

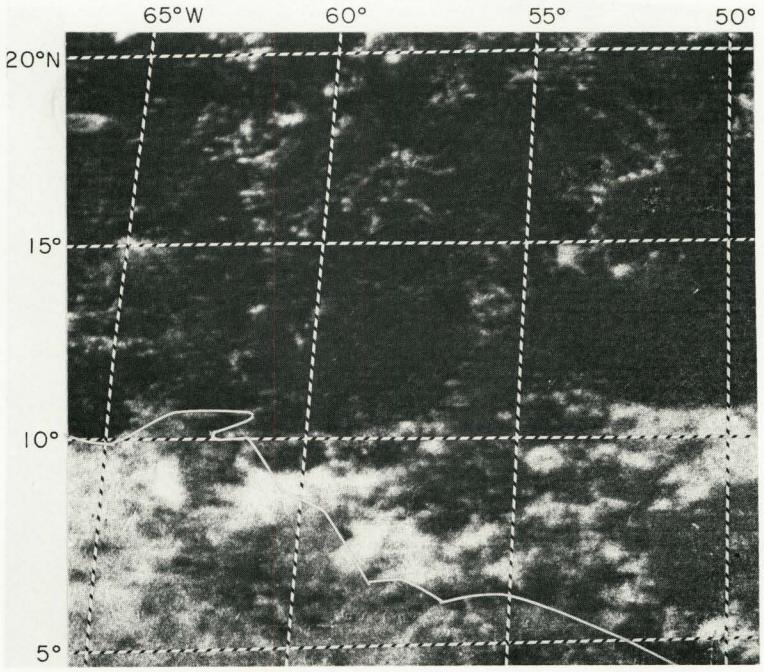

a) CLOUD COVER 1507GMT

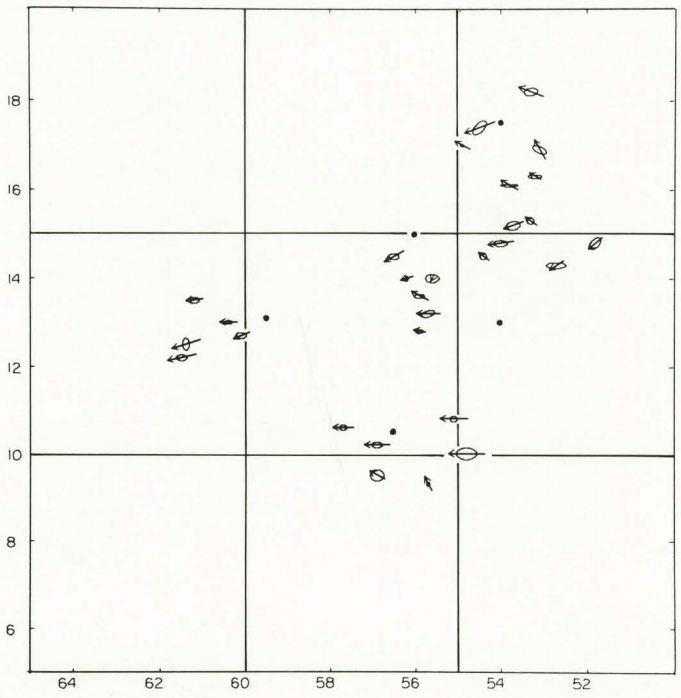

b) CLOUD MEASUREMENTS

FIGURE 24 CLOUD COVER AND CLOUD MEASUREMENTS ON 12 JULY 1969

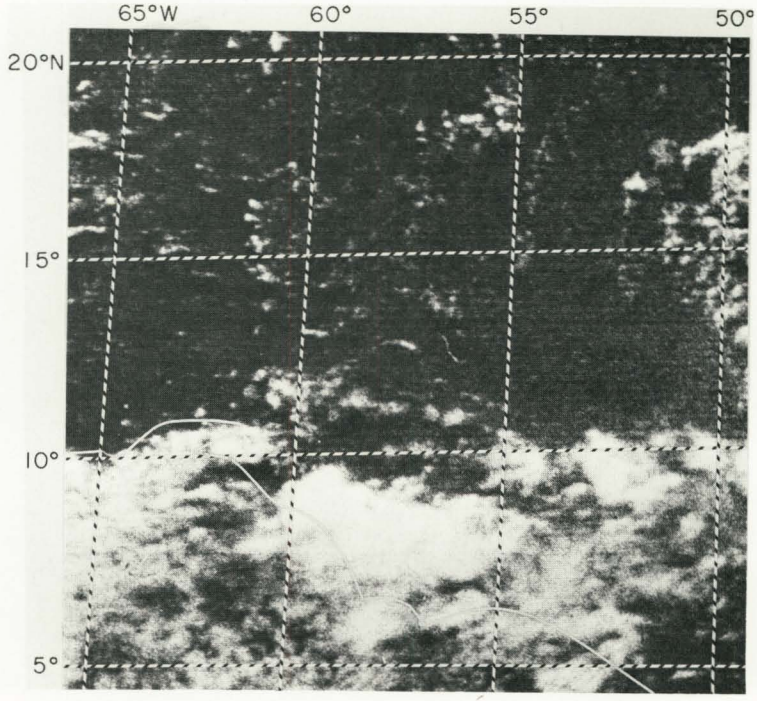

a) CLOUD COVER 1540GMT

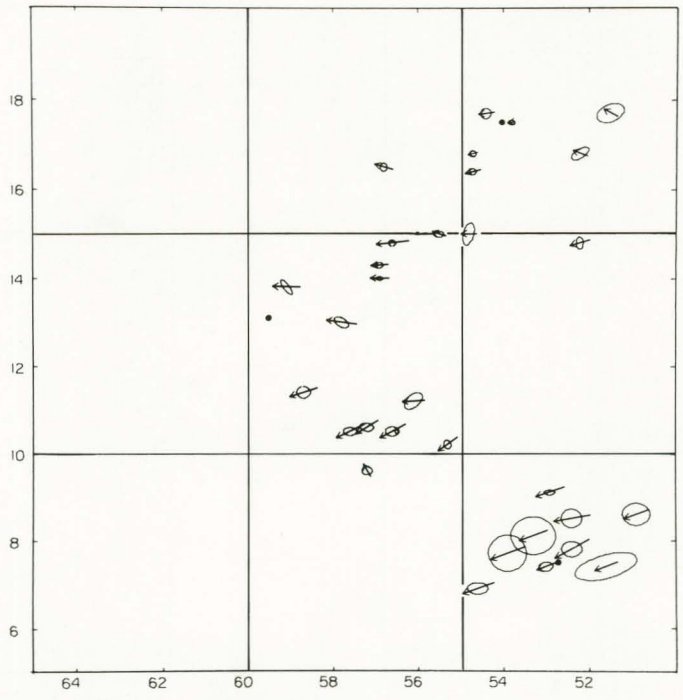

b) CLOUD MEASUREMENTS

FIGURE 25 CLOUD COVER AND CLOUD MEASUREMENTS ON 13 JULY 1969

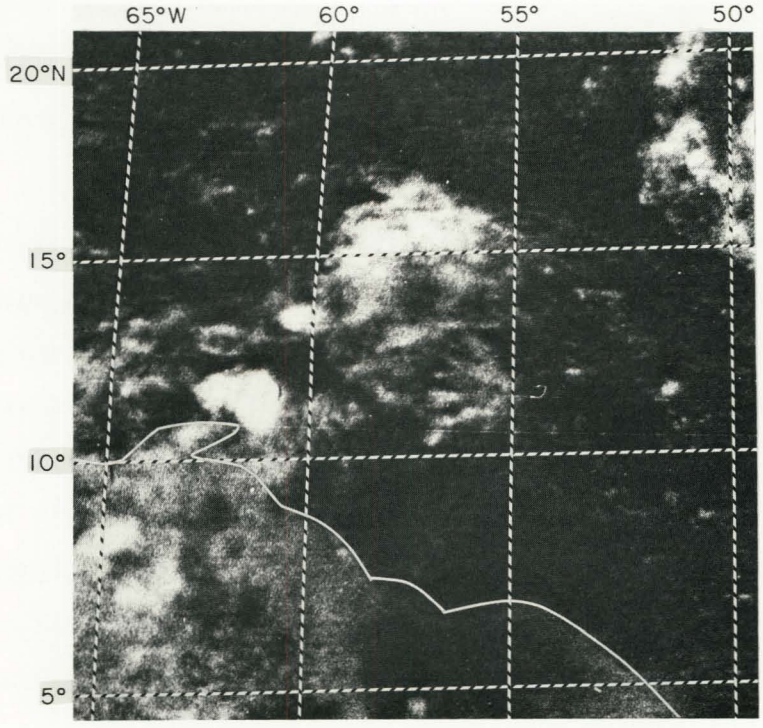

a) CLOUD COVER 1350GMT

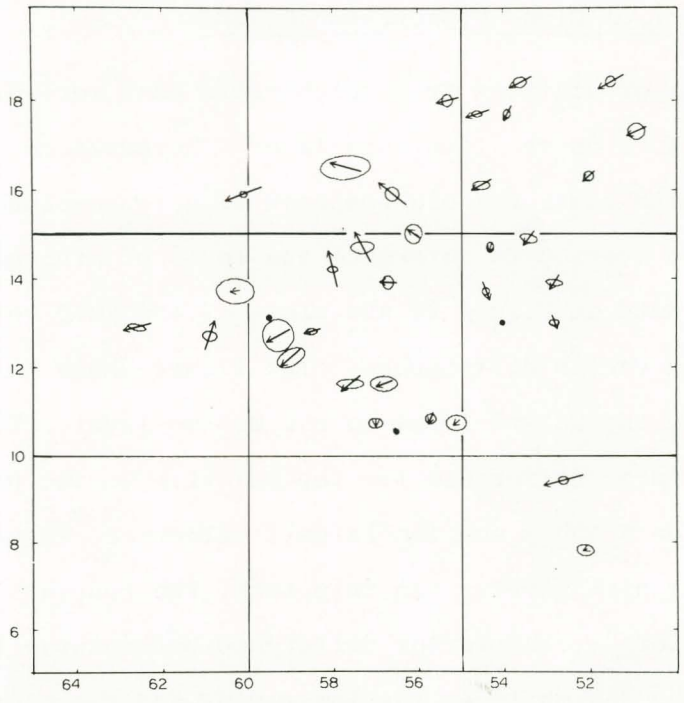

b) CLOUD MEASUREMENTS

FIGURE 26 CLOUD COVER AND CLOUD MEASUREMENTS ON 26 JULY 1969

near 15°N 57.5°W. An inverted trough was located along 50°W and the cloud cover in the northeast corner of Figure 26(a) is probably associated with this trough.

The cloud photograph for 27 July [Figure 27(a)] shows two large cloud masses now in the area. Examination of the cloud motions [Figure 27(b)] shows that the direction of motion of clouds in the vicinity of these masses varies markedly. There are northerly and southerly motions and near 16°N 59°W one cloud moved from the west. The surface chart for 1200 GMT on 27 July showed a low-pressure center near 16°N 62°W, corresponding to the cloud mass in the upper right of Figure 27(a). There was no synoptic feature in the vicinity of the area of cloud near 15°N 55°W. The cloud motion vectors, however, show no evidence of closed cyclonic circulation around the centers of the cloud masses.

B. Comparison of Cloud Motions and Rawins

Locations of stations from which rawin data were available are indicated by dots on the lower panels of Figures 24 to 27. The winds aloft from these stations were compared with those cloud motions within 120 nmi of the station to determine the level of minimum vector difference (LMVD). The dots on Figure 28 are plots of the LMVD versus the magnitude of the minimum vector differences. The figure shows that the LMVD covers the range from the 980-mb level to the 250-mb level. The magnitude of the minimum vector difference for the majority of the points on both panels is below 5 knots and the largest values are 16 knots at low levels and 8 knots at high levels. In this task, the contract called for a determination of "...the vector difference between the cloud motion and the wind at the 850-mb level for low clouds and the wind at the 300-mb level for high clouds." The arrows on Figure 28 show the change in minimum vector difference when clouds with LMVD $\leq$ 700 mb and clouds with

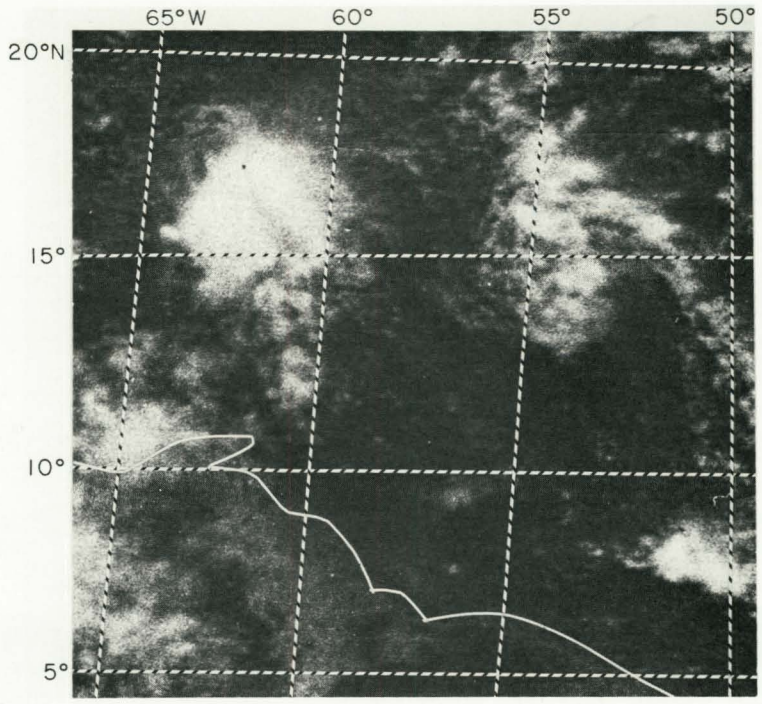

a) CLOUD COVER 1314 GMT

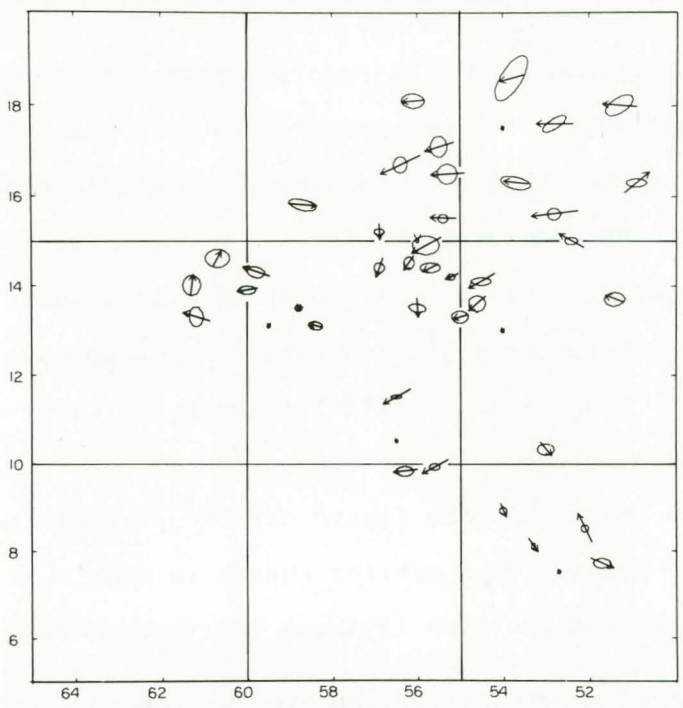

b) CLOUD MEASUREMENTS

FIGURE 27 CLOUD COVER AND CLOUD MEASUREMENTS ON 27 JULY 1969

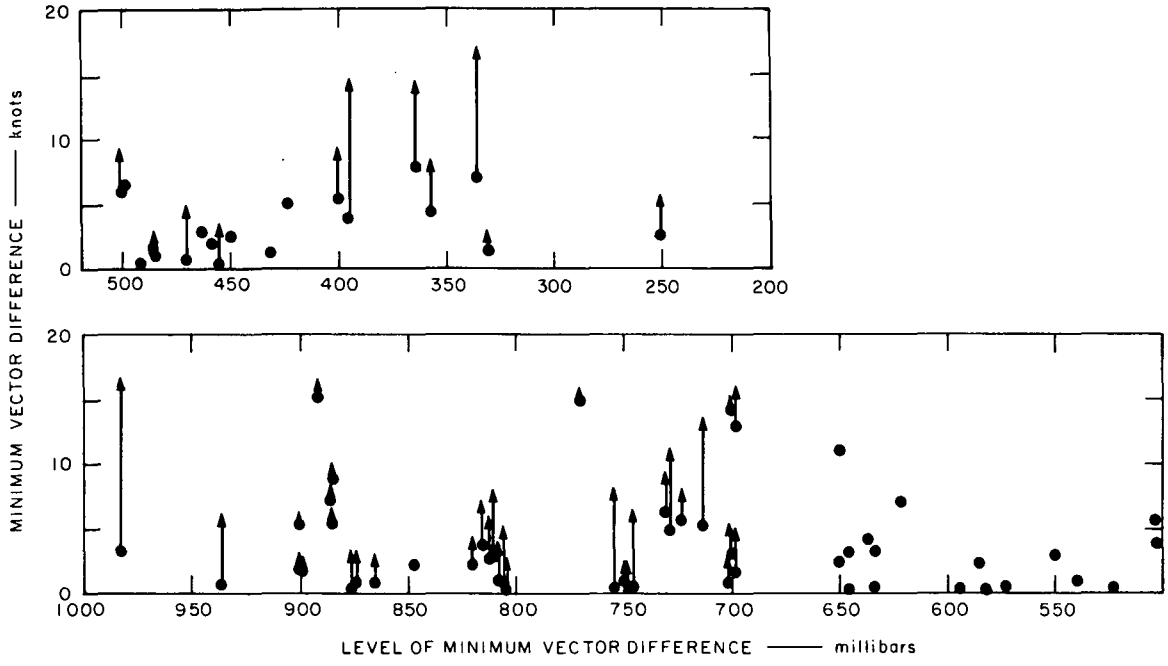

FIGURE 28 MINIMUM VECTOR DIFFERENCE AT THE LEVEL OF MINIMUM VECTOR DIFFERENCE (LMVD) AND THE CHANGE IN MINIMUM VECTOR DIFFERENCE WHEN CLOUD MOTIONS WITH LMVD AT OR ABOVE THE 500-mb LEVEL ARE COMPARED WITH 300-mb WINDS AND CLOUDS WITH LMVD AT OR BELOW THE 700-mb LEVEL ARE COMPARED WITH 850-mb WINDS (clouds between the 700- and 500-mb levels were not compared with upper or lower level winds)

LMVD $\geq$ 500 mb are compared with reported winds at the 850- and 300-mb levels, respectively. No such comparisons were made with LMVDs $>$ 700 mb and $<$ 500 mb, since these were considered as middle clouds. At levels at or above the 500-mb level the largest changes are between the 340- and 400-mb levels. At levels of 700 mb or below, there is a large change at the 980-mb level and moderate changes between the 710- and 760-mb levels. Changes are smallest through the layer from 800 to 900 mb. (They would, of course, be zero at the 850-mb level.) These results are similar to those shown by Figure 22, except that the change in magnitude is not as great. This smaller change in magnitude is probably due to more uniform wind profiles in these latitudes during the dates studied.

As mentioned previously, cloud area was one of the parameters that was computed. A scatter diagram was plotted of cloud area versus LMVD but the scatter was so large no conclusions could be drawn from the graph; therefore, it is not illustrated. The reason for plotting such

a graph was to see whether the larger clouds might move with winds at a higher level. The Thunderstorm Project (Byers and Braham, 1949) found that the diameter and height of convective cloud masses were highly correlated. Since the larger diameter clouds are taller, they should tend to move with the mean wind through a deep layer (or suffer considerable shear) and thus have a motion corresponding to winds at a higher level than the small clouds. The wide scatter in LMVD versus area showed no tendency for this to occur in the cases examined.

Cloud motion and wind at the level of minimum vector difference were compared. Figure 29 shows the result. With respect to direction, the clouds tend to move slightly to the left of the measured wind. With respect to speed, the clouds appear to move slightly faster than the measured wind. Cloud speeds greater than wind speeds at the level of minimum vector difference were also found in a previous study (Blackmer et al., 1970) using data from cloud measurements over the western United States and eastern Pacific Ocean. In the current study, deviation of cloud direction or speed from the wind direction or speed did not appear to depend on cloud size (which was coded on the original scatter diagram).

Comparison was made between cloud size, rate of change of size, and difference between cloud speed and wind speed. Figure 30 shows the results of this comparison. According to this comparison clouds with an area greater than 400 nmi^2 that were growing (positive values) generally had measured speeds in excess of the wind speed (values ranged from 2 to 6 knots) while large clouds that were decreasing in size (negative values) generally had measured speeds slower than the observed wind. No definite conclusion can be drawn from the distribution of points for the smaller clouds.

Figure 31 shows cumulative frequency curves of the magnitude of the minimum vector difference (difference between the cloud motion vector and wind vector at the level of best fit) and the difference between cloud speed and wind speed at the level of best fit. Separate

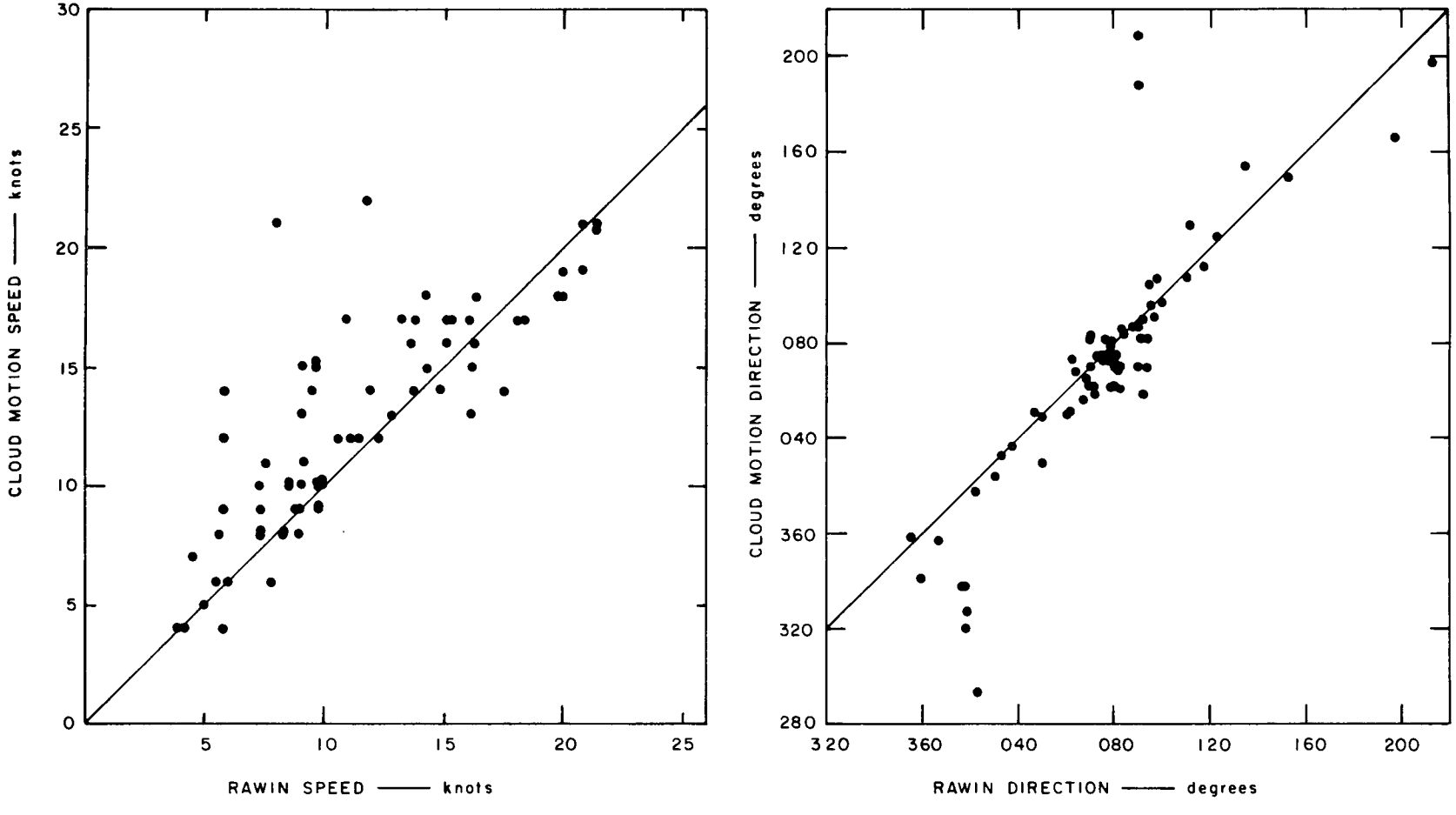

FIGURE 29 COMPARISON OF CLOUD DIRECTION AND SPEED WITH WIND DIRECTION AND SPEED AT THE LEVEL OF MINIMUM VECTOR DIFFERENCE

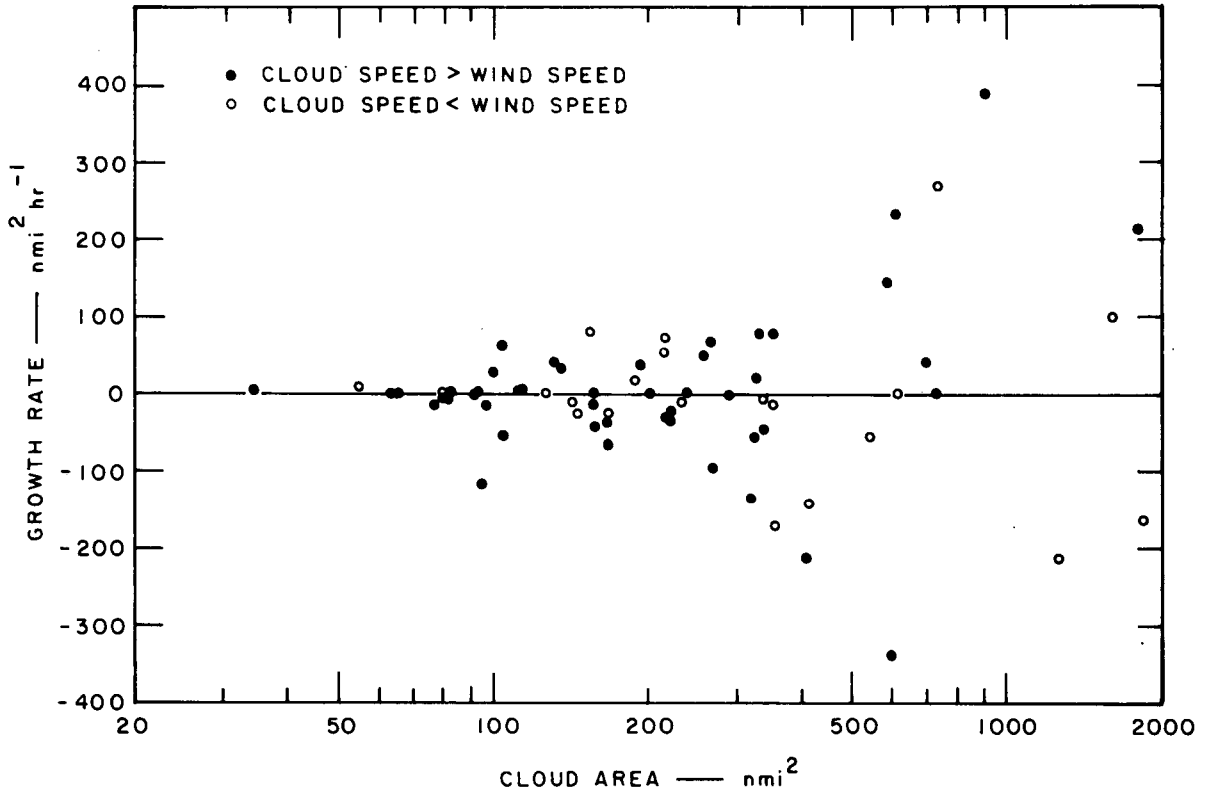

FIGURE 30 DIFFERENCE BETWEEN CLOUD SPEED AND WIND SPEED AS A FUNCTION OF CLOUD SIZE AND GROWTH RATE

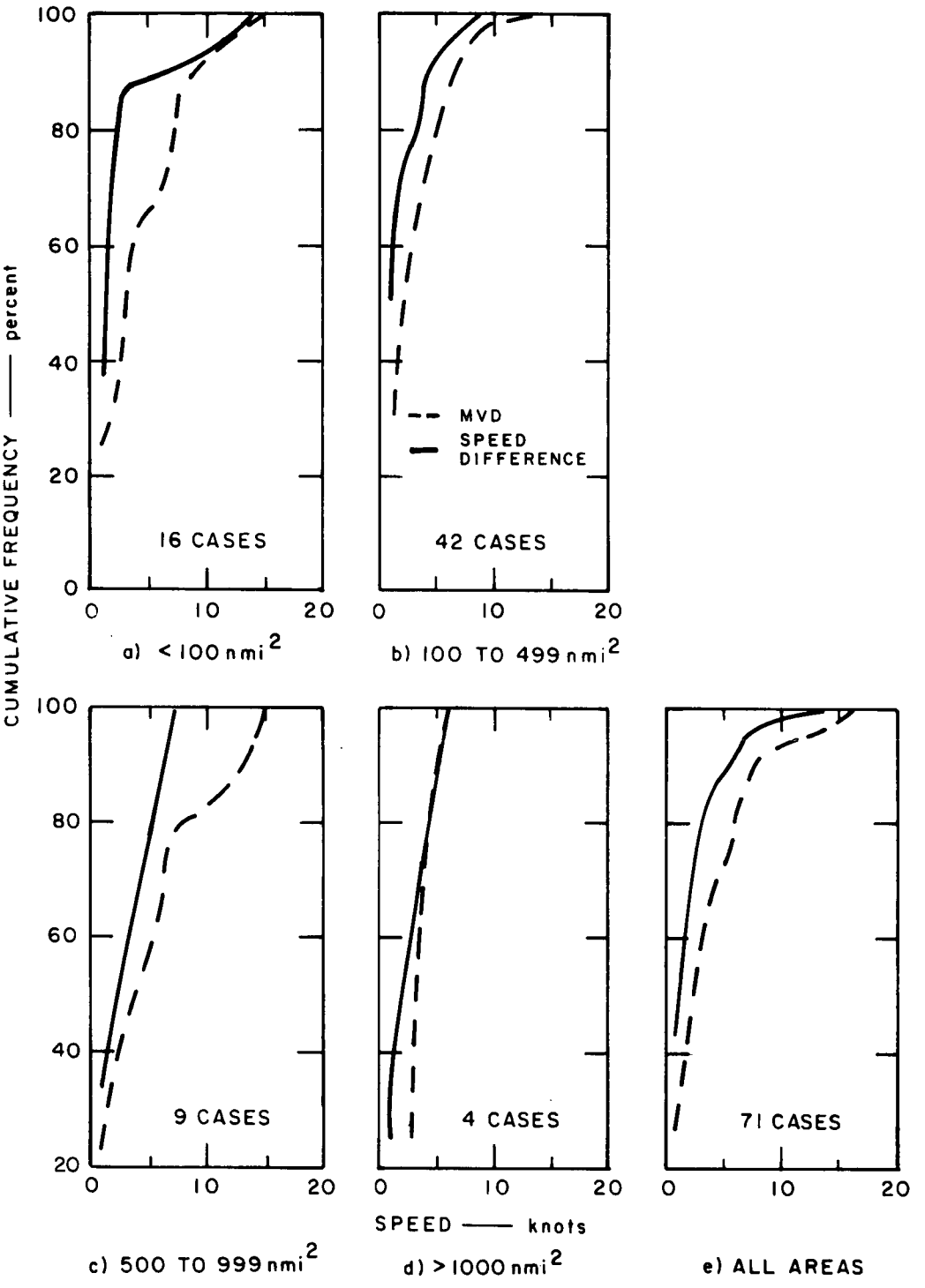

FIGURE 31 CUMULATIVE FREQUENCY OF MINIMUM VECTOR DIFFERENCE AND DIFFERENCE BETWEEN CLOUD SPEED AND WIND SPEED FOR VARIOUS SIZE CLOUDS

curves are shown for different cloud sizes. The graphs show that a substantial percent of the sample does not exceed 5 knots and that the vector difference is generally larger than the speed difference, indicating that direction difference contributes materially to the vector difference. Because of the limited number of clouds in some area categories, no definite conclusions can be drawn with respect to vector difference or speed difference as a function of cloud size.

Figure 32 shows the cumulative frequency of difference in direction between the measured cloud and observed wind at the level of best fit for clouds of various sizes. Again the sample size for some of the size categories is too small to be meaninfgul. The curve for all areas shows that 75 percent of the cloud directions were within 15° of the wind direction and only 6 percent departed more than 45° from the wind direction. The largest differences between cloud direction and wind direction is in the area class 500 to 999 nmi^2, where one difference of 119° was observed. The cloud with which this large deviation occurred was nearly 120 nmi from the closest rawin station; hence, the cloud might have been part of a circulation pattern not represented by the observed winds.

C. Summary

Measurements of cloud motion, cloud size, and growth rate were made on four days in the vicinity of rawin stations in the BOMEX network. These measurements were compared with the rawins and levels of best fit ranging from 980 to 250 mb were found. No correlation was found between cloud size and level of best fit.

The magnitude of the vector difference between the cloud motion and wind at the level of best fit was as high as 15 knots for clouds with levels of best fit below the 500-mb level and 8 knots for clouds with levels of best fit above the 500-mb level. When cloud motion vectors

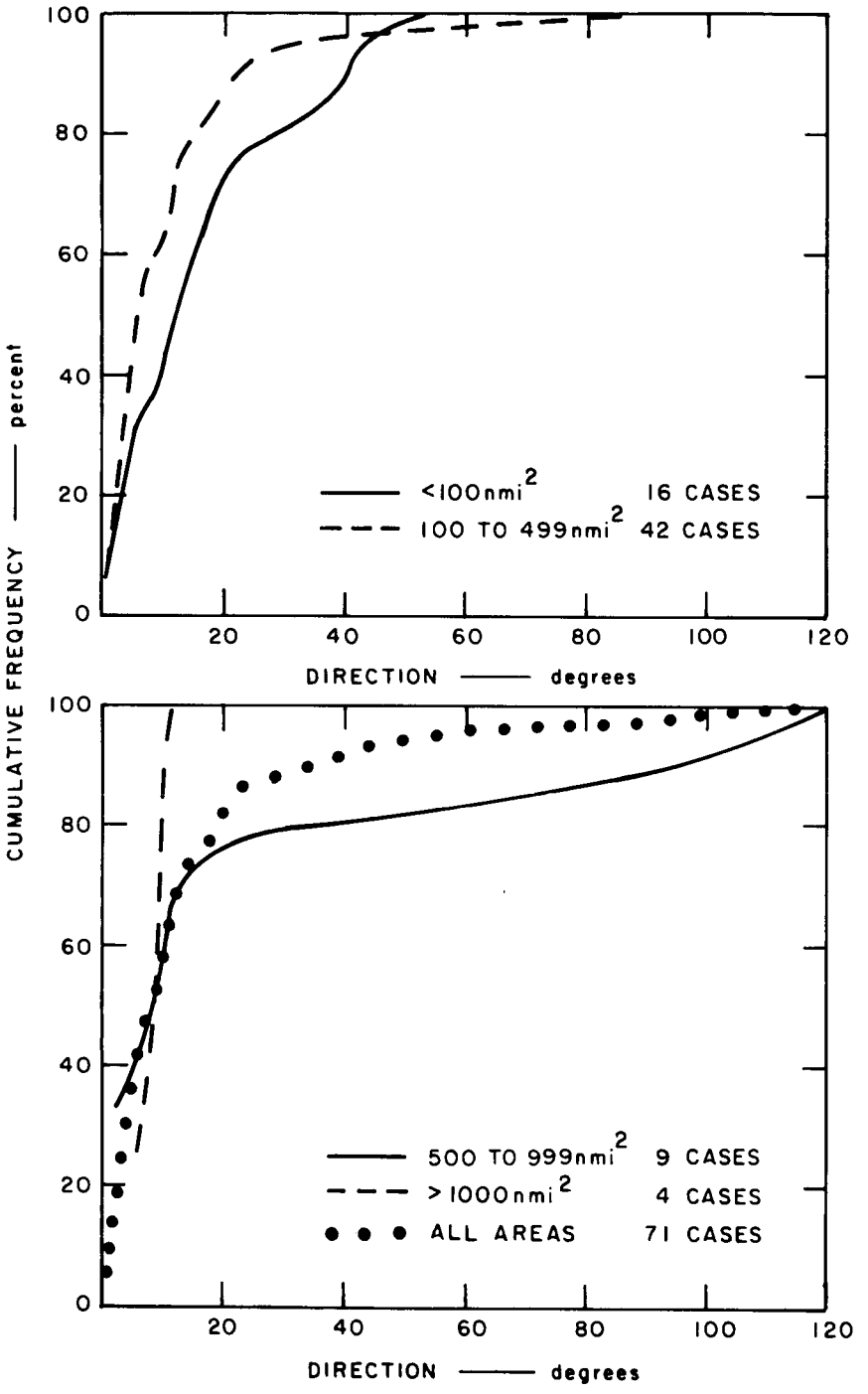

FIGURE 32 CUMULATIVE FREQUENCY OF DIFFERENCE BETWEEN CLOUD DIRECTION AND WIND DIRECTION FOR VARIOUS SIZE CLOUDS

with levels of best fit at or above the 500-mb level were compared with winds at the 300-mb level, the vector difference increased to as much as 16 knots or double the greatest minimum vector difference. When cloud-motion vectors with levels of best fit at or below the 700-mb level were compared with winds at the 850-mb level, the increases in vector difference were generally smaller than those at the higher levels.

A comparison between cloud motions and winds at the level of best fit showed that the clouds tended to move slightly faster than the observed winds and to move slightly to the left of the wind direction. This tendency did not appear to vary with cloud size. Rate of growth however, appeared to influence whether clouds moved faster or slower than the wind. Clouds with areas greater than 400 nmi^2 that were growing generally had measured speeds 2 to 6 knots in excess of the wind speed, while large clouds that were decreasing in size had measured speeds slower than the wind speed. No such tendency was observed for the smaller clouds.

No relationship between cloud size and amount of deviation from the wind direction was observed.

REFERENCES

Beers, Y., 1962, Introduction to the Theory of Error, Addison-Wesley Publishing Company, Inc.

Blackmer, R. H., Jr., E. J. Wiegman, S. M. Serebreny, and R. G. Hadfield, 1970, "Analysis of ATS Photographs Using a Specially Designed Electronic Console," Final Report-Phase I, Contract NAS5-21086, SRI Project 8244, Stanford Research Institute, Menlo Park, California.

Brodrick, J., Jr., 1969, "Some Aspects of the Vorticity Structure Associated with Extratropical Cloud Systems," ESSA Technical Memorandum NESCTM 15.

Byers, H. R. and R. R. Braham, Jr., 1949, The Thunderstorm, U.S. Government Printing Office, Washington, D.C.

Endlich, R. M., R. L. Mancuso, and H. Shigeishi, 1971, "Computation of Upper Tropospheric Reference Heights for Applying SIRS Data in Objective Analysis," Final Report, Contract 0-35199, Stanford Research Institute, Menlo Park, California.

Fujita, T. T., K. Watanabe, and T. Izawa, 1969, "Formation and Structure of Equatorial Anticyclones Caused by Large-Scale Cross-Equatorial Flows Determined by ATS-I Photographs," J. Appl. Meteor., Vol. 8, No. 4, 649-667.

Hubert, L. F. and L. F. Whitney, Jr., 1971, "Wind Estimation from Geostationary - Satellite Pictures," Mon. Wea. Rev., Vol. 99, No. 9, 665-672.

Mancuso, R. L., 1967, "A Numerical Procedure for Computing Fields of Stream-Function and Velocity Potential," J. Appl. Meteor., Vol. 6, No. 6, 994-1001.

McClain, E. P., and H. J. Brodrick, 1967, "Recent Research on the Application of Meteorological Satellite Data to Numberical Weather Analysis," Proceedings, Technical Exchange Conference, 4-7 April 1967, Air Weather Service Technical Report 196, U.S. Air Force, 42-50.

Serebreny, S. M., E. J. Wiegman, and R. G. Hadfield, 1970a, "Further Comparison of Cloud Motion Vectors with Rawinsonde Observations," Final Report, Contract E-210-69(N), SRI Project 7930, Stanford Research Institute, Menlo Park, California.

Serebreny, S. M., E. J. Wiegman, R. G. Hadfield, and W. E. Evans, 1970b, "Electronic System for Utilization of Satellite Cloud Pictures," Bull. Amer. Meteor. Soc., Vol. 51, No. 9, 848-855.

Serebreny, S. M., R. G. Hadfield, R. M. Trudeau, and E. J. Wiegman, 1969, "Comparison of Cloud Motion Vectors and Rawinsonde Data," Final Report, Contract E-193-68, SRI Project 7257, Stanford Research Institute, Menlo Park, California.

Shenk, W. E., and E. R. Kreins, 1970, "A Comparison Between Observed Winds and Cloud Motions Derived from Satellite Infrared Measurements," J. Appl. Meteor., Vol. 9, No. 4, 702-710.